EPA-600/3-75-003-a

ADAPTATION OF GAUSSIAN PLUME MODEL TO INCORPORATE MULTIPLE STATION DATA INPUT VOLUME I

by

Harvey S. Rosenblum, Bruce A. Egan,
Claire S. Ingersoll, and Michael J. Keefe

Environmental Research and Technology, Inc.
696 Virginia Road
Concord, Massachusetts 01742

Contract No. 68-02-1753
ROAP No. 21ADO-36
Program Element No. 1AA009

EPA Project Officer: D. Bruce Turner

Chemistry and Physics Laboratory
Office of Research and Development
Research Triangle Park, N. C. 27711

Prepared for

U.S. ENVIRONMENTAL PROTECTION AGENCY
Office of Research and Development
Washington, D. C. 20460

June 1975

RESEARCH REPORTING SERIES

Research reports of the Office of Research and Development, U S Environmental Protection Agency, have been grouped into series. These broad categories were established to facilitate further development and application of environmental technology. Elimination of traditional grouping was consciously planned to foster technology transfer and maximum interface in related fields. These series are:

1. ENVIRONMENTAL HEALTH EFFECTS RESEARCH
2. ENVIRONMENTAL PROTECTION TECHNOLOGY
3. ECOLOGICAL RESEARCH
4. ENVIRONMENTAL MONITORING
5. SOCIOECONOMIC ENVIRONMENTAL STUDIES
6. SCIENTIFIC AND TECHNICAL ASSESSMENT REPORTS
9. MISCELLANEOUS

This report has been assigned to the ECOLOGICAL RESEARCH series. This series describes research on the effects of pollution on humans, plant and animal species, and materials. Problems are assessed for their long- and short-term influences. Investigations include formation, transport, and pathway studies to determine the fate of pollutants and their effects. This work provides the technical basis for setting standards to minimize undesirable changes in living organisms in the aquatic, terrestrial, and atmospheric environments.

This document is available to the public for sale through the National Technical Information Service, Springfield, Virginia 22161.

Publication No. EPA-600/3-75-003-a

TABLE OF CONTENTS

		Page
1.	INTRODUCTION	1-1
	1.1 Overview	1-1
	1.2 Summary of Work Completed	1-1
2.	MODEL MODIFICATIONS	2-1
	2.1 RAM	2-1
	2.1.1 Description of Model	2-1
	2.1.2 Modifications to RAM	2-4
	2.1.2.1 Input/Output	2-5
	2.1.2.2 Selection of Significant Receptors	2-5
	2.1.2.3 Plume Rise	2-8
	2.1.2.4 Ventilation Wind	2-8
	2.1.2.5 Plume Configuration for Point Sources	2-8
	2.1.2.6 Plume Configuration for Area Sources	2-9
	2.1.2.7 Travel Time	2-11
	2.1.3 Programming Accuracy	2-13
	2.1.4 Illustrative Case Study Using RAM Modifications	2-13
	2.2 SCIM	2-22
	2.2.1 Brief Description	2-22
	2.2.2 Modifications to SCIM	2-25
	2.2.2.1 Plume Rise	2-25
	2.2.2.2 Ventilation Wind	2-25
	2.2.2.3 Plume Configuration for Point Sources	2-25
	2.2.2.4 Plume Configuration for Area Sources	2-26
	2.2.2.5 Pollutant Decay	2-28
	2.2.3 Model Case Study	2-28
	2.3 CDM	2-36
	2.3.1 Brief Description	2-36
	2.3.2 Modifications to CDM	2-38
	2.3.3 Example of CDM Run Utilizing Model Modifications	2-38

TABLE OF CONTENTS (Continued)

		Page
3.	TECHNIQUES FOR GENERATING WIND FIELDS	3-1
	3.1 Description of Methods	3-3
	3.1.1 IDPL: Inverse Distance Power Law	3-3
	3.1.2 SA: The Selective Angle Method	3-3
	3.1.3 SR: The Selective Radius Method	3-3
	3.1.4 WFM: The Weighting Factor Matrix	3-5
	3.2 Analysis of Methods	3-7
	3.2.1 Methodology	3-7
	3.2.2 Results	3-10
	3.3 Other Considerations and Guidelines for Use	3-15
4.	CONCLUSIONS AND RECOMMENDATIONS FOR FUTURE WORK	4-1
5.	REFERENCES	5-1
APPENDIX A	USER'S GUIDE TO RAM MODIFICATIONS	
	A.1 Description of Input to RAM	
	A.2 Fortran IV Program Listing	
	A.3 Test Case	
APPENDIX B	USER'S GUIDE TO SCIM MODIFICATIONS	
	B.1 Description of Input to SCIM	
	B.2 Fortran IV Program Listing	
	B.3 Test Case	
APPENDIX C	USER'S GUIDE TO CDM MODIFICATIONS	
	C.1 Description of Input to CDM	
	C.2 Fortran IV Program Listing	
	C.3 Test Case	

LIST OF ILLUSTRATIONS

Number		Page
2-1	Method of Determining Significant Receptors in RAM	2-7
2-2	Method of Estimating Cross-Wind Distance in RAM	2-10
2-3	Method of Determining Plume Path in RAM for Area Source Emissions	2-12
2-4a	Monitoring Station Locations Used in RAM Case Study	2-15
2-4b	Emissions Inventory Used for RAM Case Study	2-16
2-5	Pollutant Concentration Using Uniform Wind Field in RAM	2-17
2-6	Pollutant Concentration Using Unmodified RAM	2-18
2-7	Pollutant Concentration Using Wind Fields Shown in Figure 2-8 in Modified RAM	2-19
2-8	Wind Fields Used in RAM Case Study	2-21
2-9	Plume Path for Area Sources in SCIM	2-27
2-10	Emissions Inventory Used in SCIM Case Study	2-29
2-11	Emissions Inventory; Meteorological Station and Receptor Locations Used in CDM Case Study	2-40
3-1	Selective Angle Method	3-4
3-2	Selective Radius Method	3-6
3-3	Observation Point and Calculation Point Configurations	3-8
3-4	Uniform Gradient Analytical Wind Fields	3-9
3-5	Potential Flow Field	3-14

1. INTRODUCTION

This report describes the results of a program conducted by Environmental Research & Technology, Inc. (ERT), under contract to the United States Environmental Protection Agency (EPA) (Contract No. 68-02-1753) entitled Adaptation of Gaussian Plume Model to Incorporate Multiple Station Data Input.

1.1 Overview

The most commonly used procedure for the evaluation of air pollution control strategies is based on mathematical modeling of the atmospheric dispersion of pollutants through air quality simulation models. The meteorological data input most frequently used for multiple-source urban air pollution models is oversimplistic in that the dispersion processes over an entire urban area are assumed to be adequately described by meteorological observations at one point such as a neighboring airport or National Weather Service Forecast Office. At the present time air quality sampling networks are being established where wind observations are available at many locations in the same urban area such as the St. Louis Regional Air Pollution Study (RAPS) network. Also, the prediction of detailed wind patterns is the objective of numerical mesoscale models presently under development. Numerical dispersion models, which are well-suited for incorporating the output of these models or other spatially and time varying data into calculations of pollutant concentration, may be too demanding in terms of computer time and input data requirements to be practical for many studies or routine use. It is, therefore, desirable to extend the usefulness of Gaussian-plume models by adapting them for multi-station input data. Because of this consideration and the need to improve the accuracy of air quality simulation models, a contract for the incorporation of several modifications and potential improvements into standard Gaussian-plume urban dispersion models was awarded.

1.2 Summary of Work Completed

Urban dispersion models provided by EPA were modified to consider multiple station information on wind speed and direction. Three models

were modified: the Real-Time Air-Quality-Simulation Model (RAM) and the Sampled-Chronological Input Model (SCIM), both short-term models, and the Climatological Dispersion Model (CDM) a long-term model. Relatively straightforward modifications were studied, ones which are useful, practical approximations rather than formulations that are absolutely consistent in a mathematical sense. The modifications had two basic objectives: the first, to develop techniques for describing wind conditions at any point within a region in which arbitrarily-located observing stations exist; and second, to identify critical points in the dispersion algorithms at which the additional multiple-station wind data could be incorporated and to modify these computation routines accordingly. The modifications were compared among themselves on the basis of accuracy, computational efficiency and ease of use. Although no observational data was available to verify the various approaches, the results of applications to hypothetical meteorological situations indicate that more realistic results can be obtained by the incorporation of multiple-station data.

The following sections describe the work performed including model modifications and analysis methods. Section 2 describes the modifications made in the EPA models and examples of case studies which illustrate the changes. The techniques developed for generating wind fields from arbitrarily-located observation points are detailed in Section 3. An analysis of the accuracy and computational efficiency of each method is given. In addition, guidelines are presented so that the most applicable methods can be selected for a specific situation.

2. MODEL MODIFICATIONS

The following sections describe the modifications made to the EPA models. Since they involve the effect of horizontal wind variability on plume dispersion, techniques were developed that develop wind fields from observations at arbitrarily spaced locations. The nature of the wind generator techniques is critically important because they affect the model results equally as much as the dispersion algorithm changes themselves. In this section it is assumed that wind information on speed and direction is readily available whenever needed; the following section describes the manner in which this information is produced.

A brief review of the highlights and main features of each model is given. For a more complete description, the reader is referred to the original user's manuals in these programs.

2.1 RAM

2.1.1 Description of Model

RAM is a version of the Gaussian plume model that estimates pollutant concentrations from both area and point sources for periods of several hours to one day. It provides model values of one-hour concentrations at receptors. A series of consecutive hourly observations of wind direction, wind speed, atmospheric stability, mixing depth and temperature is used for input. The calculation of hourly concentrations assumes steady-state conditions for each hour that are independent of previous or future conditions. The average pollutant concentration for the period is then calculated by averaging the modeled hourly concentrations. The principal limitation of the model is the restriction of its use to inert pollutants in regions of relatively smooth terrain. The former limitation to conditions, where the designation of a single wind vector is accurate, is eliminated by modifications described later in this report.

Pollutant concentrations due to emissions from large stationary or "point" sources is given by standard Gaussian plume equations:

For stable conditions or unlimited mixing,

$$\chi_p = \frac{Q}{2\pi u \sigma_y \sigma_z} \exp\left[-\frac{1}{2}\left(\frac{y}{\sigma_y}\right)^2\right]\left\{\exp\left[-\frac{1}{2}\left(\frac{z-H}{\sigma_z}\right)^2\right] + \exp\left[-\frac{1}{2}\left(\frac{z+H}{\sigma_z}\right)^2\right]\right\}; \quad (2\text{-}1)$$

For unstable or neutral conditions and $\sigma_z > 1.6\ L$,

$$\chi_p = \frac{Q}{2\pi \sigma_y L u} \exp\left[-\frac{1}{2}\left(\frac{y}{\sigma_y}\right)^2\right] \quad (2\text{-}2)$$

For other conditions:

$$\chi_p = \frac{Q}{2\pi u \sigma_y \sigma_z} \exp\left[-\frac{1}{2}\left(\frac{y}{\sigma_y}\right)^2\right]\left\{\exp\left[-\frac{1}{2}\left(\frac{z-H}{\sigma_z}\right)^2\right] + \exp\left[-\frac{1}{2}\left(\frac{z+H}{\sigma_z}\right)^2\right]\right\} \quad (2\text{-}3)$$

$$+ \sum_{N=1}^{N=J} \left\{\exp\left[-\frac{1}{2}\left(\frac{z-H-2NL}{\sigma_z}\right)^2\right] + \exp\left[-\frac{1}{2}\left(\frac{z+H-2NL}{\sigma_z}\right)^2\right] + \exp\left[-\frac{1}{2}\left(\frac{z-H+2NL}{\sigma_z}\right)^2\right] + \exp\left[-\frac{1}{2}\left(\frac{z+H+2NL}{\sigma_z}\right)^2\right]\right\}$$

χ_p = concentration due to point sources, g m^{-3}

Q = emission rate, g sec^{-1}

u = wind speed, m sec^{-1}

σ_y = horizontal standard deviation of plume width; function of travel time, stability, m

σ_z = vertical standard deviation of plume depth; function of travel time, stability, m

y = receptor crosswind distance from plume centerline, m

z = receptor height, m

H = effective plume height, m

L = mixing depth, m

The summation is terminated when successive terms contribute a specified small amount to the total. Area source contributions are determined from

$$\chi_a = Q_a \int_0^{T_1} \frac{\chi u}{Q_\ell} \, dt \qquad (2\text{-}4)$$

χ_a = concentration due to area sources, g m^{-3}

Q_a = area source strength, g m^{-2} sec^{-1}

Q_ℓ = line source strength for line source of infinite crosswind strength, g m^{-1} sec^{-1}

T_1 = travel time between source-receptor pair, sec

The integrand is determined from the following equations:
For stable or unlimited mixing conditions;

$$\frac{\chi u}{Q_\ell} = \frac{1}{\sqrt{2\pi}\,\sigma_z} \left\{ \exp -\frac{1}{2}\left[\frac{z-H}{\sigma_z}\right]^2 + \exp -\frac{1}{2}\left[\frac{z+H}{\sigma_z}\right]^2 \right\} \qquad (2\text{-}5)$$

If $\sigma_z > 1.6\ L$; and

$$\frac{\chi u}{Q_\ell} = \frac{1}{L} \qquad (2\text{-}6)$$

For all other conditions;

$$\frac{\chi u}{Q_\ell} = \frac{1}{\sqrt{2\pi}\,\sigma_z} \exp \left\{ -\frac{1}{2}\left[\frac{z-H}{\sigma_z}\right]^2 + \exp -\frac{1}{2}\left[\frac{z+H}{\sigma_z}\right]^2 \right.$$

$$+ \sum_{N=1}^{N=J} \left[\exp\left(-\frac{1}{2}\left(\frac{z-H-2NL}{\sigma_z}\right)^2\right) + \exp\left(-\frac{1}{2}\left(\frac{z+H-2NL}{\sigma_z}\right)^2\right) \right.$$

$$\left. \left. + \exp\left(-\frac{1}{2}\left(\frac{z-H+2NL}{\sigma_z}\right)^2\right) + \exp\left(-\frac{1}{2}\left(\frac{z+H+2NL}{\sigma_z}\right)^2\right) \right] \right\} \qquad (2\text{-}7)$$

The term z is the receptor height. The value of J in Equation 2-7 is determined as in Equation 2-3.

The integration of Equation 2-4 is complicated in the multiple station case by the variation of wind speed, u, with location. As a result, the travel time, T = x/u, where x is distance, varies with downwind distance. The modification developed to account for this is described later.

The narrow plume hypothesis (Calder, 1971) is utilized to select those area sources that affect pollutant concentrations at the receptor for which calculations are being made. The integration of Equations 2-5, 2-6 and 2-7 in RAM is accomplished at the outset of the program. The results are stored for fixed values of the travel time T. Pollutant concentrations for values of T are determined by interpolation between the stored values.

The dispersion parameters σ_y and σ_z are functions of downwind travel time of the form AT^B where A, and B are empirical constants dependent upon travel time and atmospheric stability.

Many of the computational schemes were designed by Turner and Hrenko (1974) so that RAM could be used on a real-time basis in an inexpensive manner. For this reason computational efficiency and model input simplicity were highly desirable. The method described above for integrating Equation 2-4 for fixed travel times and interpolating between them and a scheme for establishing significant receptors at the locations of expected maximum concentrations that uses the resultant wind as guidance are directed to this objective. The model includes the use of Brigg's (1971) plume rise, a power law to express the vertical variation of wind speed, identification of the most significant point and area source contributions, flexible input and output, and card punching for contour mapping.

2.1.2 Modifications to RAM

The following areas were modified in RAM:

- Input/Output
- Selection of Significant Receptors

- Plume Rise
- Ventilation Wind
- Plume Configuration for Point Sources
- Plume Configuration for Area Sources
- Travel Time

2.1.2.1 Input/Output

The format of RAM's input data was altered to incorporate the extra data required in the multi-station model. The details of the changes such as data type, column numbers and sequence are described in Appendix A. It is sufficient to mention here that wind data from the monitoring locations and the height of each instrument are required for model input and are listed in the output. One value per hour of mixing depth, atmospheric stability class and temperature is assumed to be representative of the entire region.

The tabulation of model results remains the same except that a summary of the hourly inputs from the several station locations is listed for each hour. In addition, the resultant wind at each observation point is given where appropriate.

2.1.2.2 Selection of Significant Receptors

RAM selects two additional receptor locations for each significant point source (the point sources whose emissions exceed a pre-specified level) and one location for each significant area source where maximum concentrations are expected to occur as a result of each source's pollutant emission during the period. The source-receptor geometry is determined by the resultant wind for the period. The receptor is placed at distance x_{max} downwind where

$$x_{max} = uT_{max} \qquad (2\text{-}8)$$

where

x_{max} = downwind distance at which maximum concentration is expected to occur

T_{max} = travel time to x_{max}

u = wind speed

T_{max} is calculated from

$$T_{max} = aH^b \tag{2-9}$$

where

H = effective height of source, assuming $u = 3$ m sec^{-1}

a,b = empirical constants which are functions of the type of source (point or area), H, and the modal stability class for the period.

For a point source the significant receptors are located at travel times of T_{max} and $2T_{max}$ from the source location. For area sources the significant receptor is placed downwind of the area source center as determined by the travel time T_{max} from the intersection of the resultant wind azimuth with the source boundary.

In the multiple station case both the distance downwind of the source as well as the azimuth of the resultant wind are changed because the resultant wind is a function of location. The selection of significant receptors must take this into account in order for this part of the program to retain its original purpose of identifying locations of expected maximum concentration. The approach developed to handle this situation is shown in Figure 2-1 in which significant receptors R_1 and R_2 are selected downwind from point source P. This is done by first using the wind at P to determine point A at distance

$$x_{max} = T_{max} |u_p| \tag{2-10}$$

The resultant wind at point B, the midpoint of line segment PA, is then used as the approximate average wind along the path trajectory starting

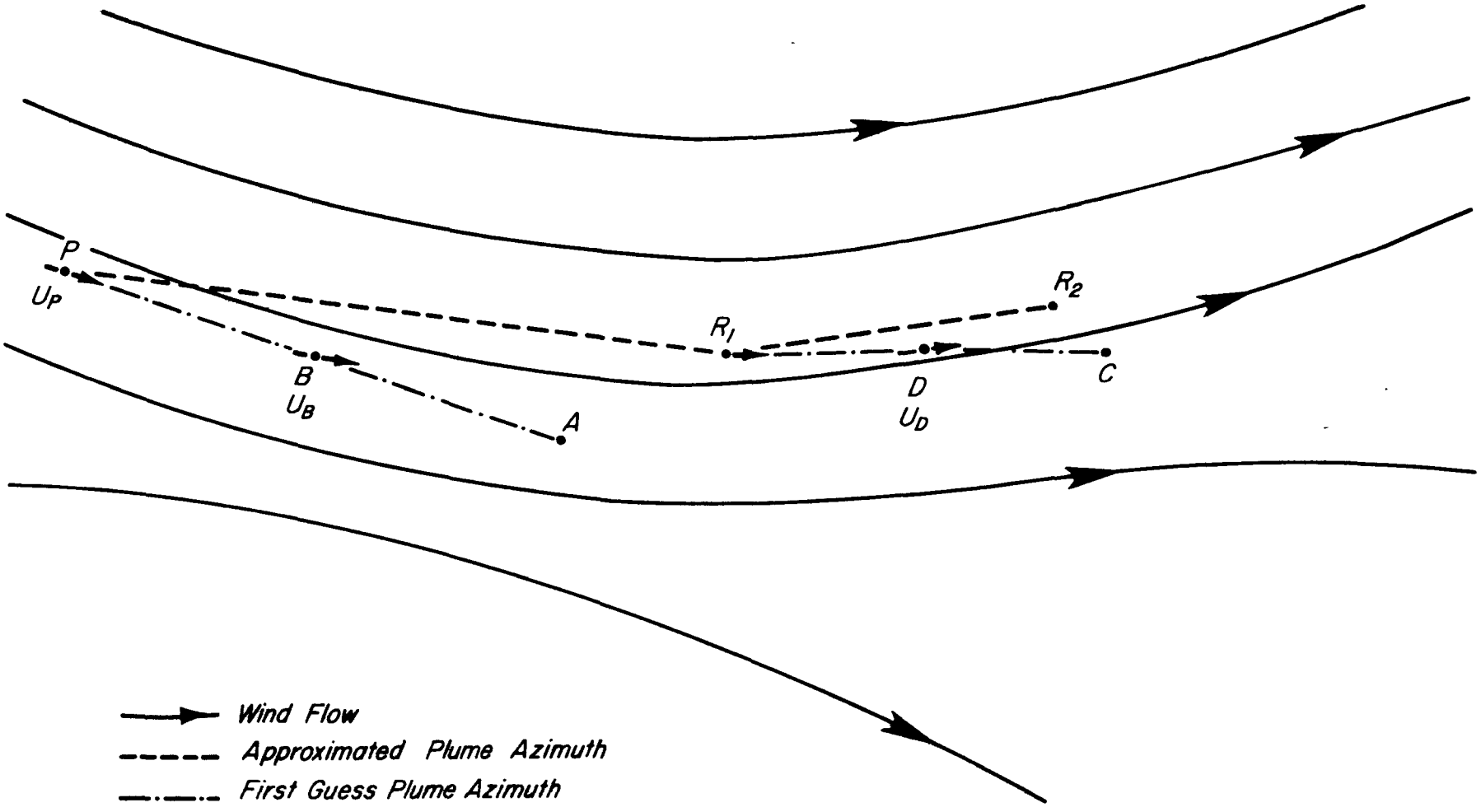

Figure 2-1 Methods of Determining Significant Receptors, R_1 and R_2, Downwind of Point Source P in RAM - Wind vectors at B and D, the midpoints of line segments PA and R_1C, are used to determine R_1 and R_2.

at P. Point R_1 is thus defined as the receptor location at distance $|u_p|T_{max}$ downwind from P in the direction of u_B. Since RAM selects a second significant receptor for each point source at distance $x = 2x_{max}$, the process is repeated starting at point R_1, to determine the location of R_2 in the multi-station case. The resultant wind u_D at point D, the midpoint of line segment R_1C, is used to determine R_2. The procedure for selecting the appropriate significant receptor downwind of an area source case is similar with point P denoting the area source center. Only one receptor is selected at distance x_{max} for area sources.

2.1.2.3 Plume Rise

Brigg's plume rise is modified so that the wind speed at the source is used when wind speed is involved in the calculation. The speed at the source is determined by field generator techniques for each point source considered and hence varies from source to source.

2.1.2.4 Ventilation Wind

The wind speed term in the denominator of Eqs. 2-1, 2-2 and 2-3 is sometimes referred to as the ventilation wind speed. This term is the same quantity that is used to calculate plume rise. Emissions emanating from a source will be diluted by the mixing of ambient air with the effluent gases. The rate at which this occurs will be different for each source in the multiple-station case because the wind speed varies from location to location. The change implemented in RAM to account for this is the replacement of the ventilating wind speed by a horizontally varying value which is evaluated at each source separately.

2.1.2.5 Plume Configuration for Point Sources

The trajectory of a plume emitted in an atmosphere of varying winds will be curved. Plume configuration can be approximated by a series of straight lines joined end to end. The accuracy of this type of plume path is a function of the length of each line segment and the curvature of the wind field; an exact replication of the plume path can be obtained if infinitesimally small line segments are used. However, the calculation of crosswind and downwind distance, necessary for Gaussian-plume models, becomes very complicated and computationally expensive for large

emissions inventories. Therefore, the approximate scheme (shown in Figure 2-2) was developed which would be valid for the majority of cases encountered on the urban area scale. This scheme is most applicable to situations where the wind field varies uniformly between the source-receptor pair so that the wind conditions at the mid-point of a line joining the two is an approximation of the wind conditions between the two locations.

In Figure 2-2 the wind direction at the midpoint of a line segment joining the point source-receptor pair of interest is used to determine point C, the distance of closest approach of the plume to R. From C the cross-wind distance y_R is determined. Note that the dotted segment PC is not the expected plume centerline but a reasonably close approximation of the actual plume path in Figure 2-2. It appears that this kind of approximation is reasonably accurate in wind fields that vary uniformly over the distance between the source and the receptor and is expecially appropriate for receptor locations relatively close to the actual trajectory centerline (where the contribution from an upwind source is most significant).

2.1.2.6 Plume Configuration for Area Sources

The method of successive approximation is also used to determine the contribution from area sources. In the single-station version of RAM only those area sources lying directly upwind of a particular receptor are considered in the calculation of pollutant concentration. This feature remains in the multi-station case, except that the upwind direction is a curved path and varies from place to place. Because of the neglect of crosswind dispersion in the area source calculations, it is feasible to describe the upwind direction as a multi-segmented path and avoid the mathematical complexity that would be involved in the point-source calculations. The bends in the path are made at the intersections with area source boundaries because it is at these points that the integral in Eq. 2-4 is evaluated. By utilizing the average wind speed and direction between the receptor and the successive boundaries of area sources, the location of each intersection and the travel time from the intersection to the receptor can be calculated.

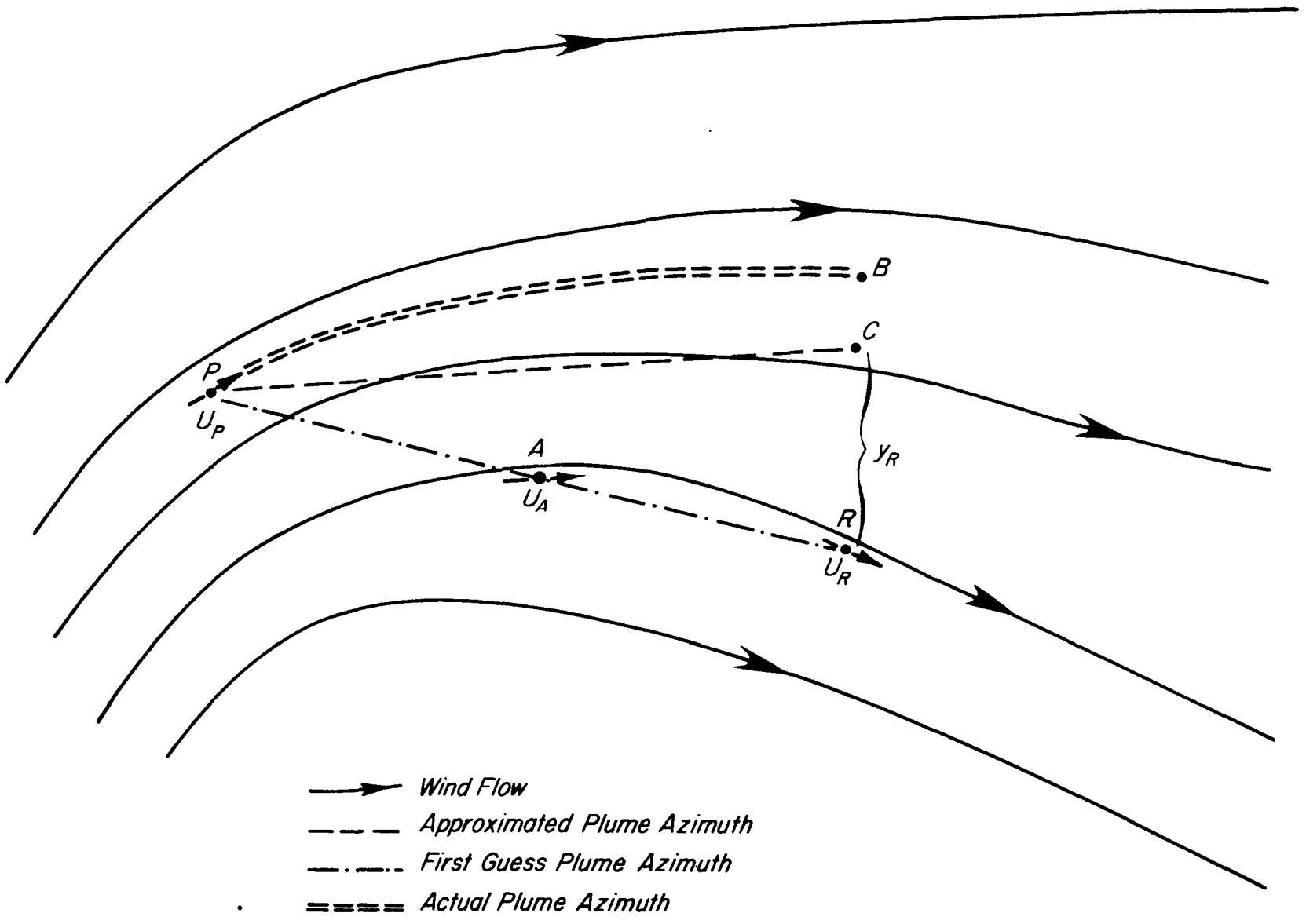

Figure 2-2 Method of Estimating Cross-Wind Distance, y_r, from Plume Centerline to Receptor R in RAM, for Plume Originating at Source P - Wind vectors are given by U_i (i = P,A,R).

In Figure 2-3, the wind directions at the receptors, R_E and R_I in the diagram, are used to determine the first guess upwind intersection point with the area source boundaries, B and H in the diagram. The wind conditions at the midpoint of these segments, A and G respectively, are used to determine new intersection points, C and H, and the travel times along the segments. The process is repeated from intersection point to intersection point and traces a multi-jointed plume path. From the information on travel time, it is possible to determine area source contributions as before from the tabulation of integral values from Eq. 2-4 stored internally. For instance, the contribution C from area source III to pollutant concentration at point R_E, is given by

$$C = Q_{III}\left[\left(\frac{\chi}{Q_{III}}\right)T_F - \left(\frac{\chi}{Q_{III}}\right)T_C\right]$$

where

Q_{III} = area source III strength

T_F = travel time from point F to R_E

T_C = travel time from point C to R_E

The values of the ratio $\frac{\chi}{Q}$ are stored internally for specified values of T. The evaluation of $\frac{\chi}{Q}$ at other points is done by linear interpolation on the stored values.

2.1.2.7 Travel Time

Since RAM uses plume travel time to determine the diffusion parameters, σ_y and σ_z, it is necessary to estimate the average wind speed over the plume path. In the multi-station case, where the wind speed can be expected to vary from place to place, an exact determination of travel time would require a sophisticated iterative algorithm. Since such a scheme would be used repeatedly during the course of a diffusion calculation, a fair amount of computer time would be involved. With such factors in mind, an approximation similar to that described in the two previous sub-sections was adopted. The wind speed at the midpoint

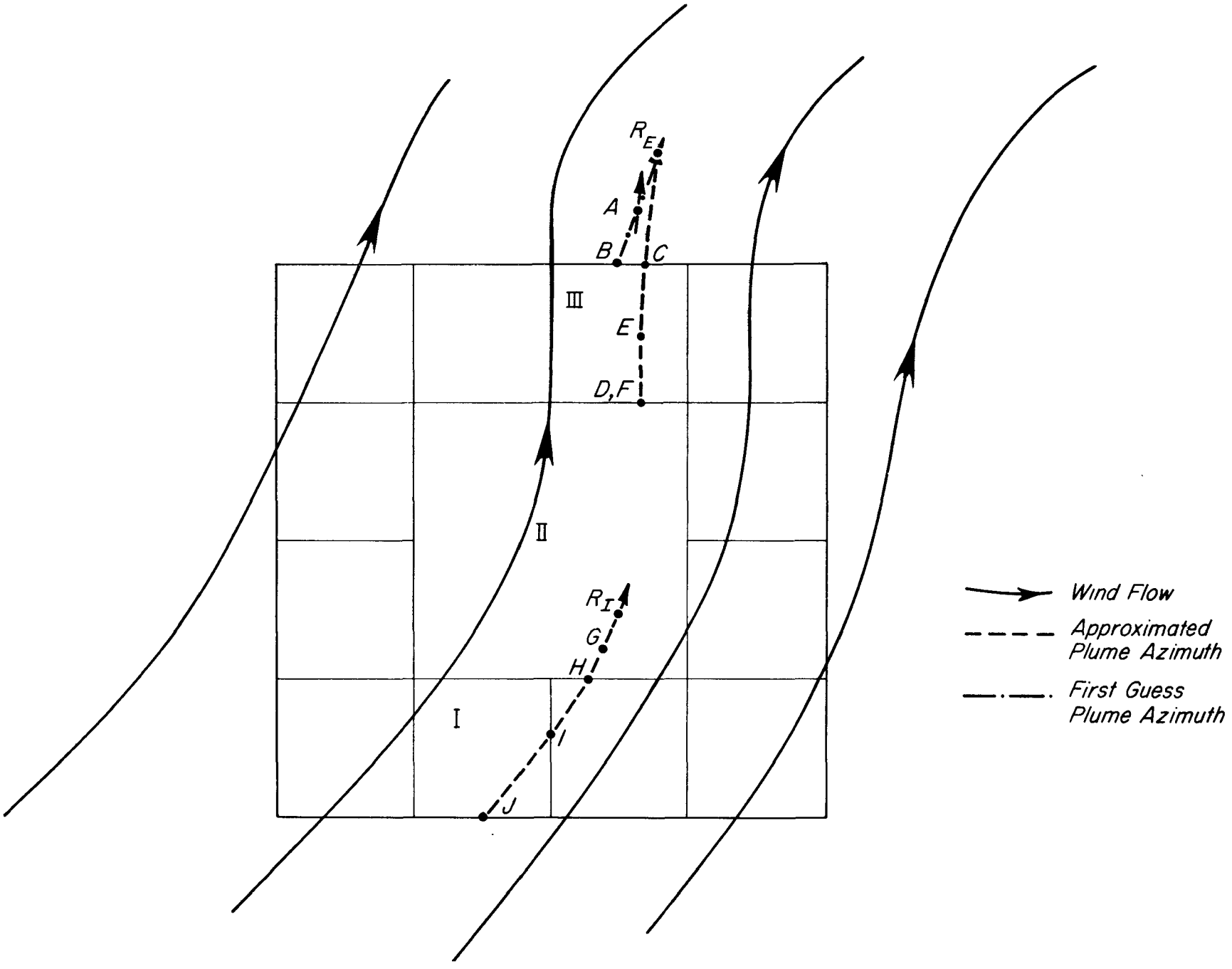

Figure 2-3 Method of Determining Plume Path in RAM for Area Source Emissions - R_E and R_I are receptor points external and internal to the area source grid. The wind vectors at A,E and G, the mid-points of first guess plume paths, are used to determine final plume path.

of the source-receptor pair is used as the average wind speed over the path taken by the plume centerline, segment PC in Figure 2-2 and $R_E C$, CF, $R_I H$, etc., in Figure 2-3. Thus travel time T in Figure 2-2 is

$$T = \frac{PC}{|U_A|} \tag{2-11}$$

The wind speed $|U_A|$ is modified by a power-law relationship to give wind speed at stack level if stack height exceeds 10 m.

2.1.3 Programming Accuracy

In order to check programming accuracy, a comparison of unmodified and modified RAM runs was made using the identical meteorological and emissions data input. In the unmodified version the meteorological input took the form of a single wind direction and wind speed; in the modified version the comparable input consisted of 25 observing points being assigned the same wind parameters. The accuracy check was extended to include multiple station input utilizing each of the four objective analysis techniques for generating wind fields discussed in Section 3. In all cases the final version of the modified RAM produced modeled pollutant concentrations identical to those produced by the original, unmodified program.

2.1.4 Illustrative Case Study Using RAM Modifications

The modified RAM was applied to meteorological conditions simulating a sea breeze phenomenon to illustrate the more realistic results produced by the multiple-station model. The selective angle method was used with a selection angle of 45 degrees (see Section 3.1.2). The meteorological input consisted of wind speed and direction from 25 stations over a 21-hour period. For comparison RAM was run for the same period using wind data from only one of the 25 stations. The results clearly show the advantage of diffusion calculations which incorporate multi-station data when the wind varies significantly over an area.

The locations for the 25 monitoring stations were assigned by superimposing the configuration of the St. Louis RAPS network on a square grid 30 kilometers on a side (Figure 2-4a). The coordinates of the stations are given in Table 2-1. For the single-station case, only wind data from station 16 near the center of the grid was used. The emissions inventory used is shown in Figure 2-4b.

Figure 2-5 shows SO_2 concentrations resulting during hour one. The wind field is uniform across the region with a 10 meter per second wind at 315 degrees. This pattern represents both the single and multiple station cases.

In subsequent hours the wind direction turns until at most stations it is in the range 180 to 220 degrees immediately prior to the onset of the sea breeze. A comparison of multi-station and single-station model runs for hour 18, shown in Figures 2-6a and 2-7a respectively, reveals a close similarity between the two since the wind directions at most stations are within 60 degrees of each other (the wind field is shown in Figure 2-8). The multiple-station case shows a narrower band of concentrations since Station 23, the most eastern station, has a wind direction of 90°, indicating the edge of flow reversal.

During hour 19 the sea breeze front has penetrated to Station 16 (Figure 2-8), and the wind has shifted to an easterly direction there. The single station case produces isopleths of SO_2 shown in Figure 2-5. All pollutant material is transported to the west, and a pattern of pollutant concentration markedly different from that of the previous hour results. Because the meteorological conditions for hours 20 and 21 are unchanged at Station 16, the concentration patterns for hours 20 and 21 for the single-station case are almost identical to that shown for hour 19 and are not shown again. For the multiple-station case, the concentration patterns for hours 18, 19, 20 and 21 show the effect of the sea breeze's progress across the grid (Figure 2-7). The transition from hour to hour is uniform and smooth. A band of high concentrations is found in the vicinity of the sea breeze front, where the northeastward movement of emitted material is prevented by the easterly flow in the eastern part of the grid.

TABLE 2-1

LOCATIONS OF MONITORING STATIONS FOR THE RAM SEA BREEZE SIMULATION

Station Number	Coordinates x	y
1	14.82	13.89
2	14.34	15.90
3	15.96	14.70
4	15.81	13.02
5	14.64	12.78
6	13.02	13.20
7	13.56	14.82
8	16.32	17.49
9	18.57	13.77
10	15.75	11.58
11	13.02	11.55
12	11.52	14.31
13	12.84	17.16
14	15.06	19.59
15	18.72	19.20
16	20.94	17.01
17	20.04	11.43
18	14.31	8.52
19	10.08	11.01
20	8.07	16.05
21	11.25	21.30
22	14.61	30.00
23	25.53	15.66
24	16.14	0
25	0	15.09

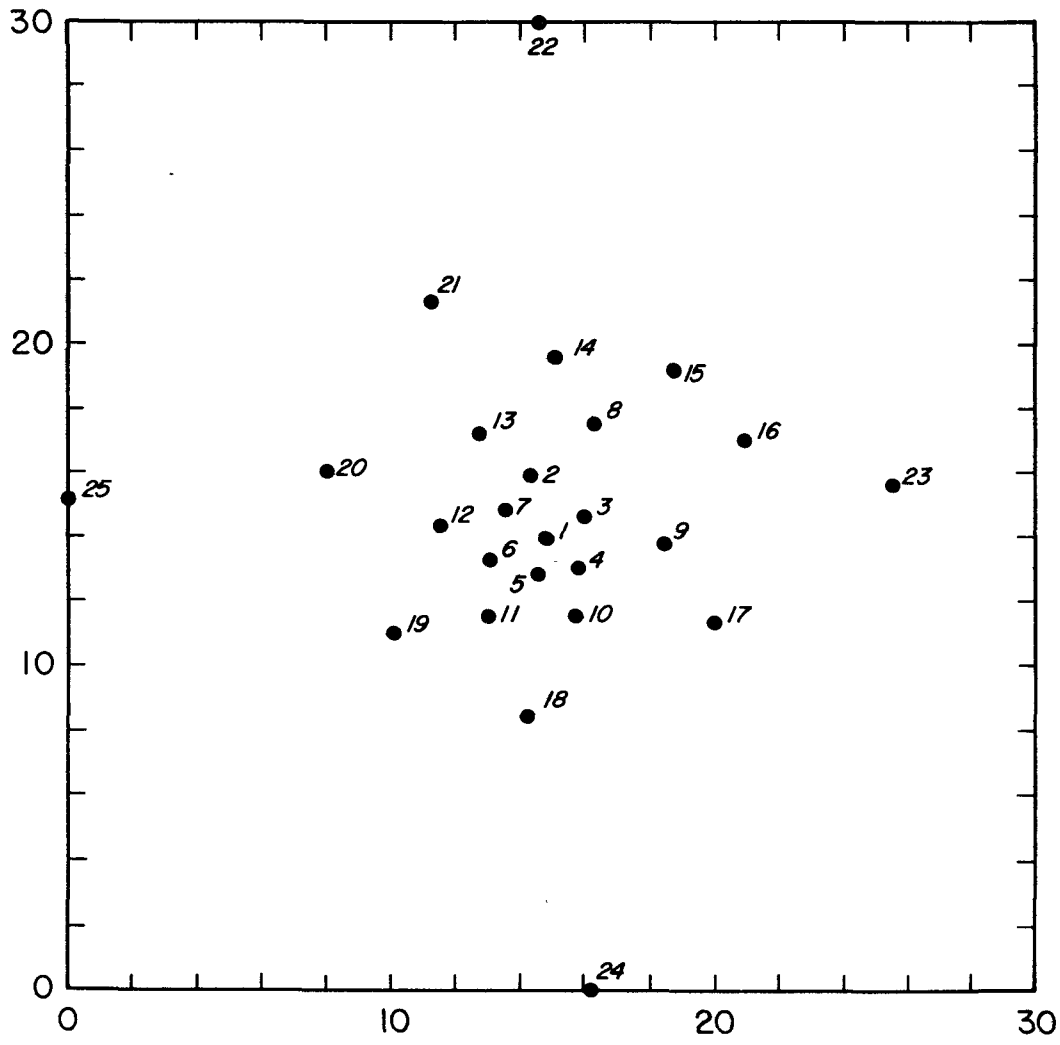

Figure 2-4a Monitoring Station Locations Used in RAM Case Study

Point Sources

	Emission Rate (g/sec)	Ht. (m)
P1	4987.50	200.
P2	997.50	100.
P3	997.50	100.
P4	997.50	100.
P5	199.50	50.

Area Sources

	Emission Rate ($g/m^2/sec$)	Ht. (m)
A1	3.9375×10^{-7}	0.0
A2	3.9375×10^{-6}	15.0
A3	3.9375×10^{-6}	20.0
A4	3.9375×10^{-6}	15.0
A5	3.9375×10^{-6}	20.0
A6	3.9900×10^{-5}	25.0
A7	3.9375×10^{-7}	0.0

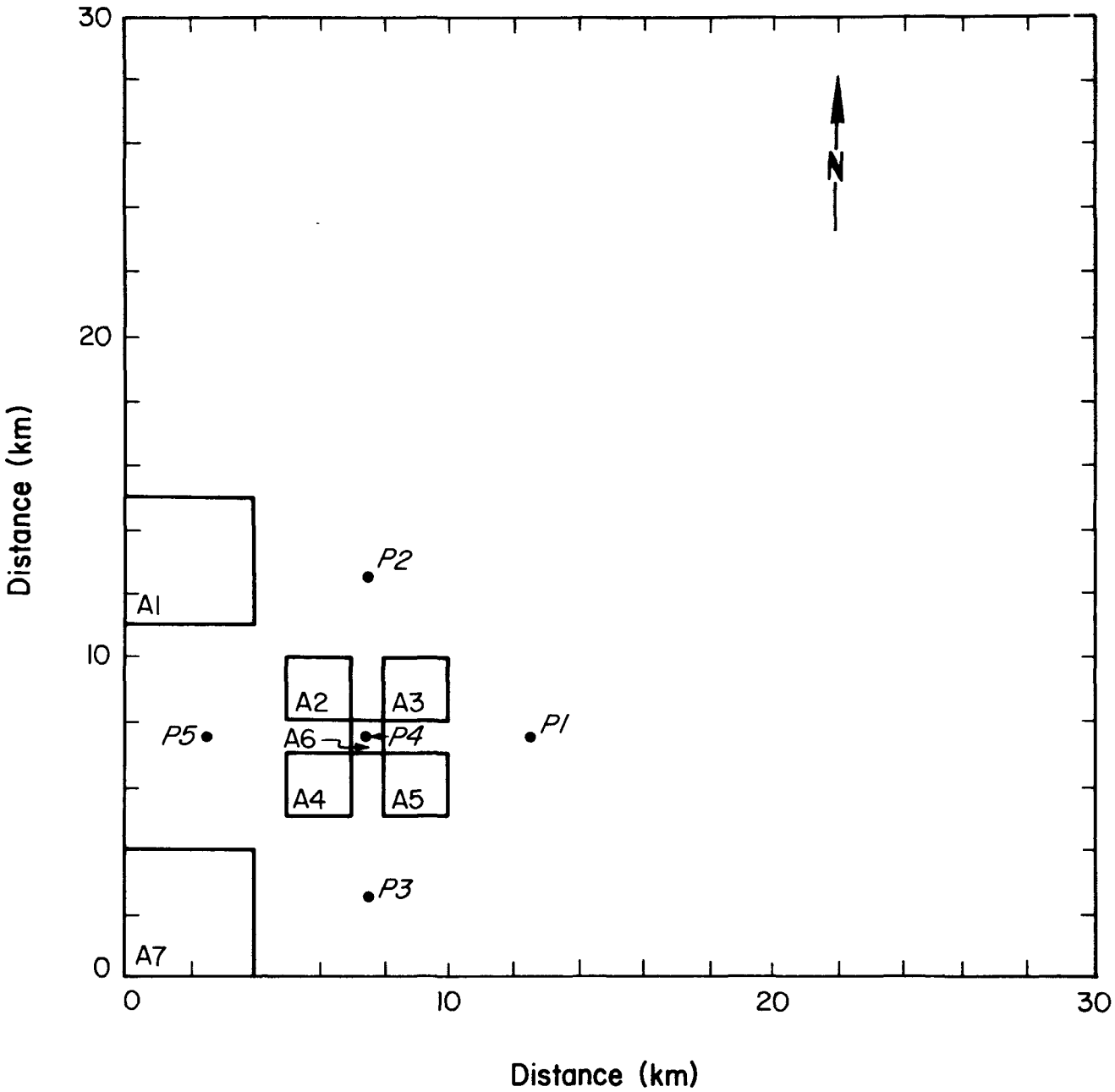

Figure 2-4b Emissions Inventory used for RAM Case Study

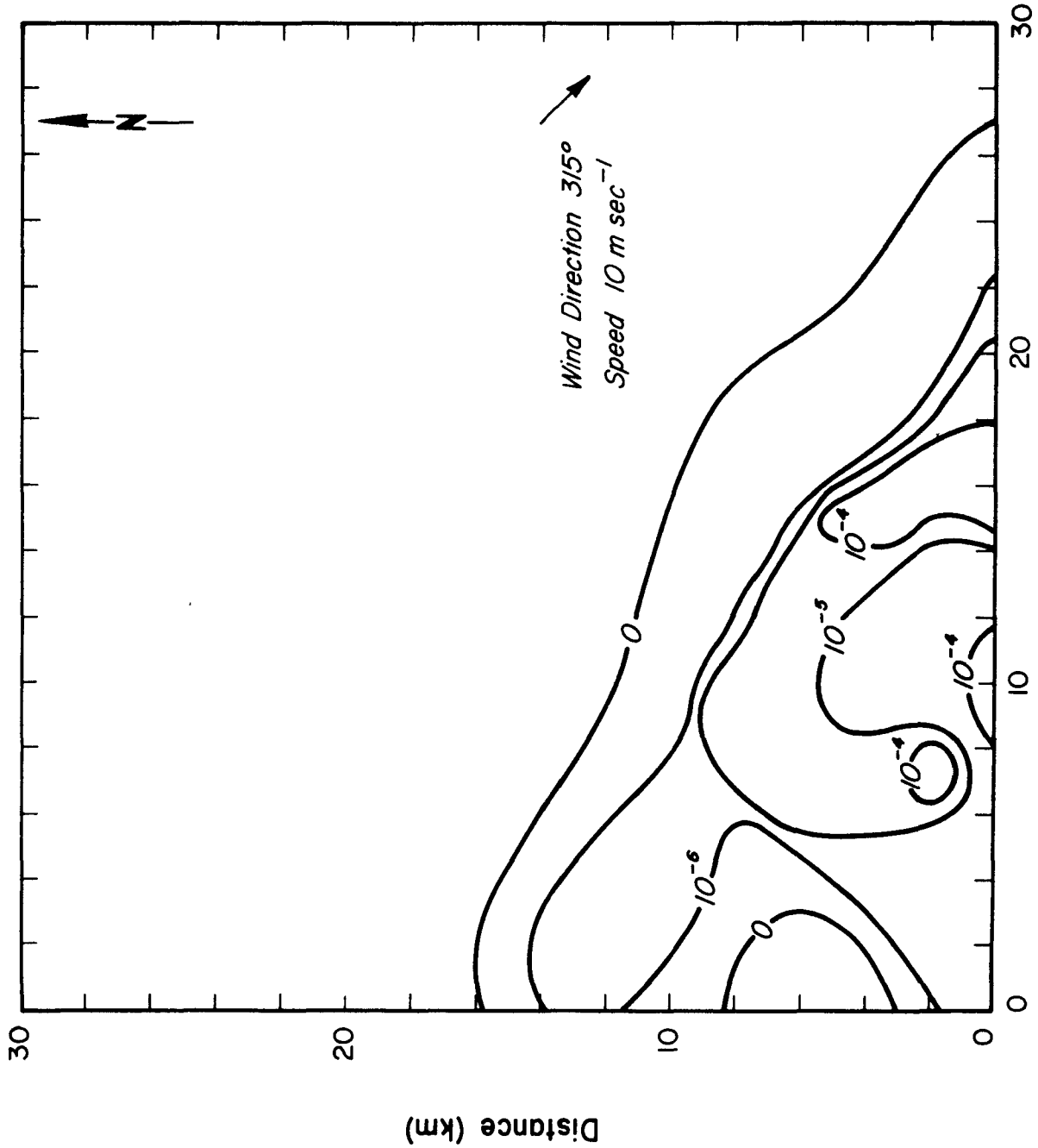

Figure 2-5 Pollutant Concentration (g m^{-3}) using a Uniform Wind Field in RAM

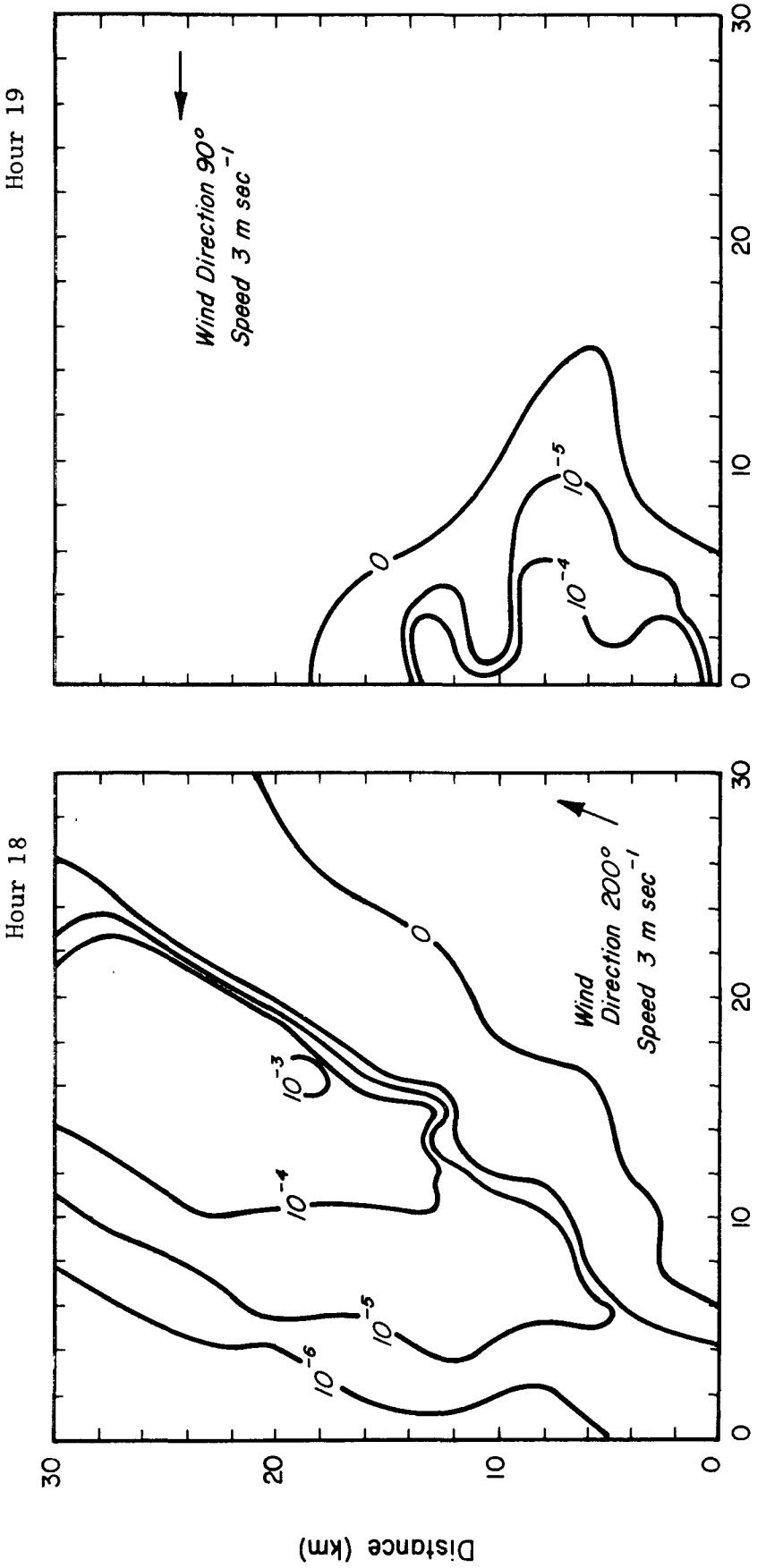

(a) Wind Direction of 200°

(b) Wind Direction of 90°

Figure 2-6 Pollutant Concentrations ($g\ m^{-3}$) using Unmodified RAM

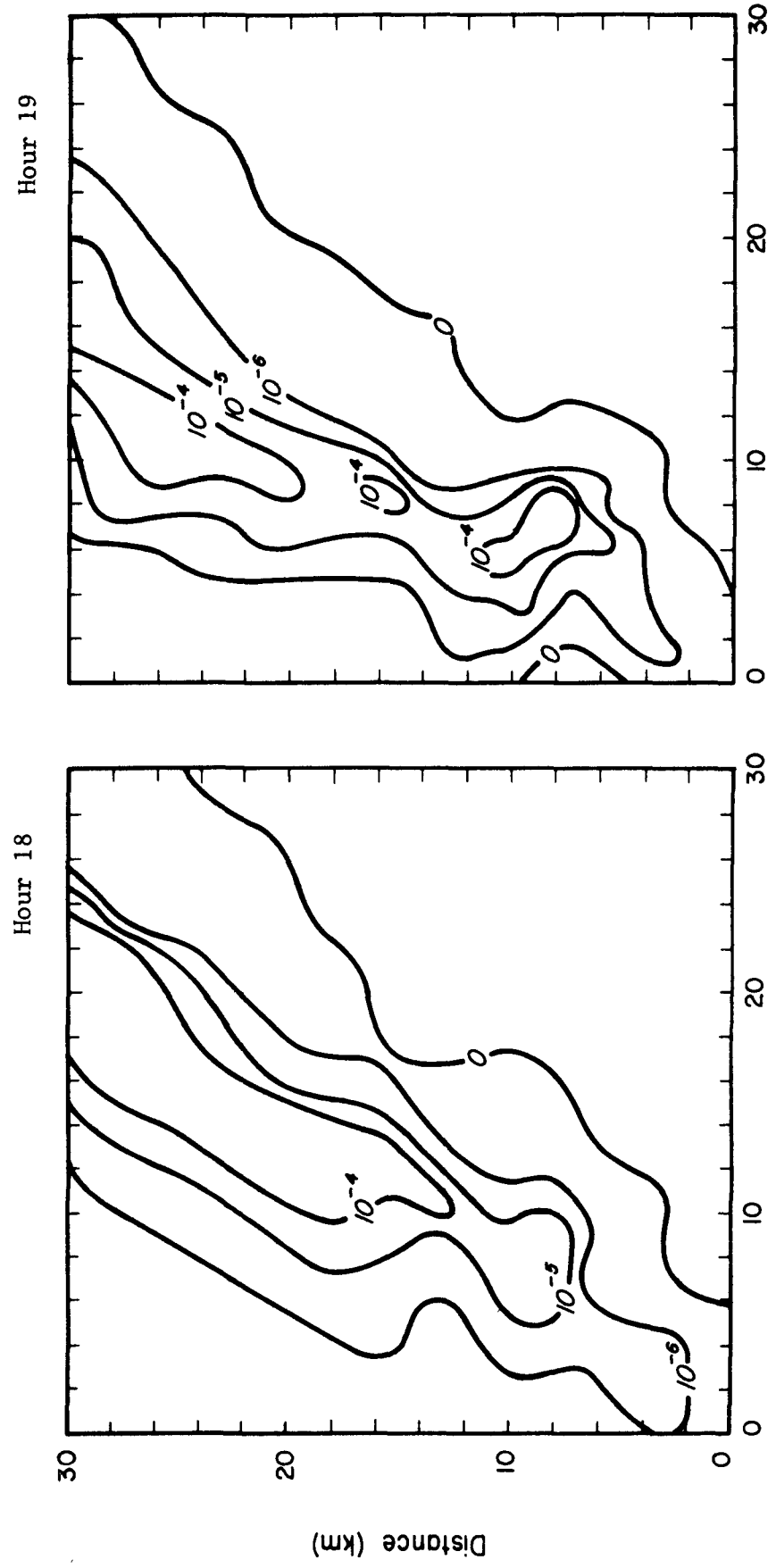

Figure 2-7 Pollutant Concentration (g m^{-3}) using the Wind Fields shown in Figure 2-8 in Modified RAM

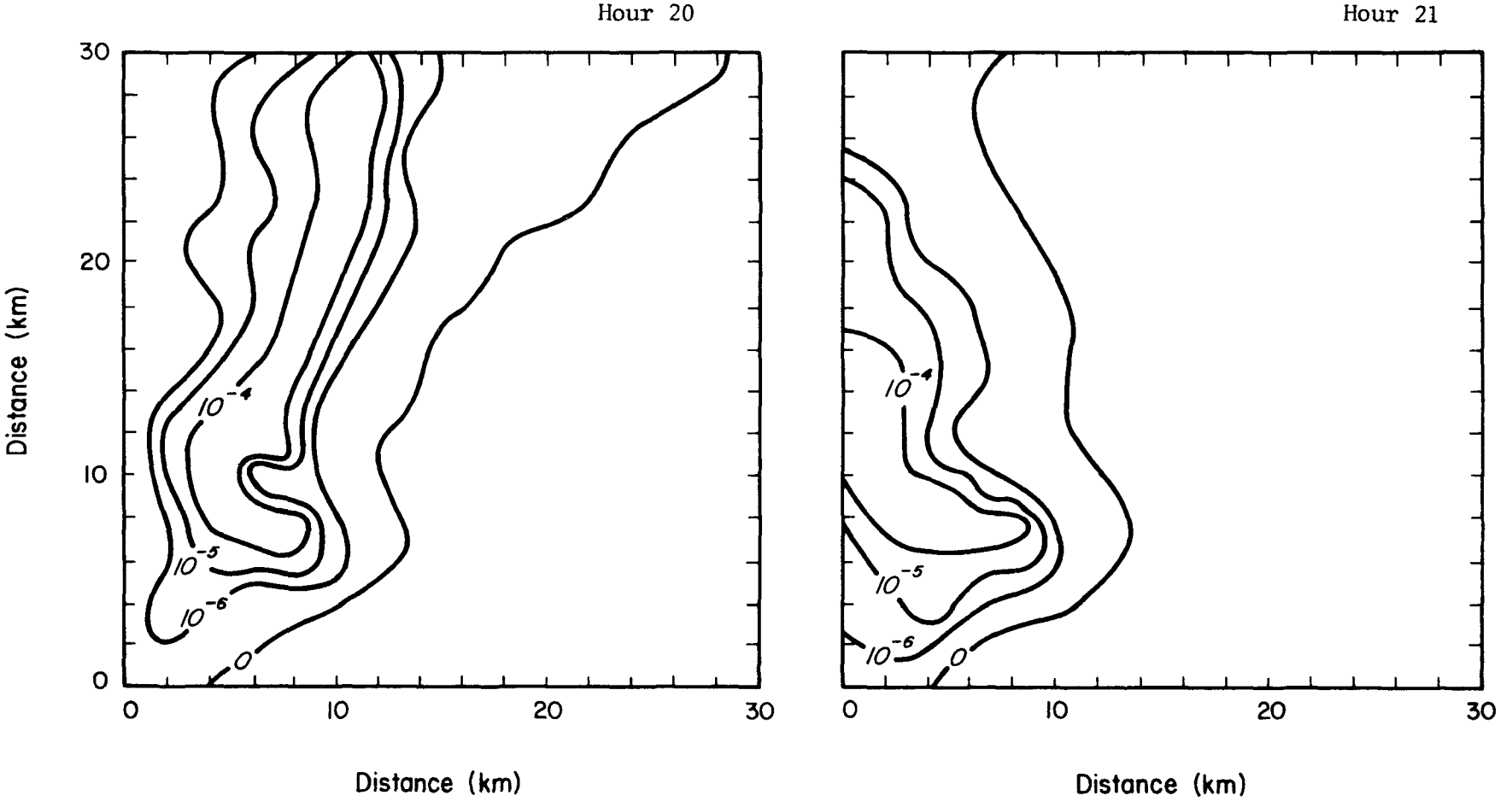

Figure 2-7 Pollutant Concentrations (g m^{-3}) using the Wind Fields shown in Figure 2-8 in Modified RAM

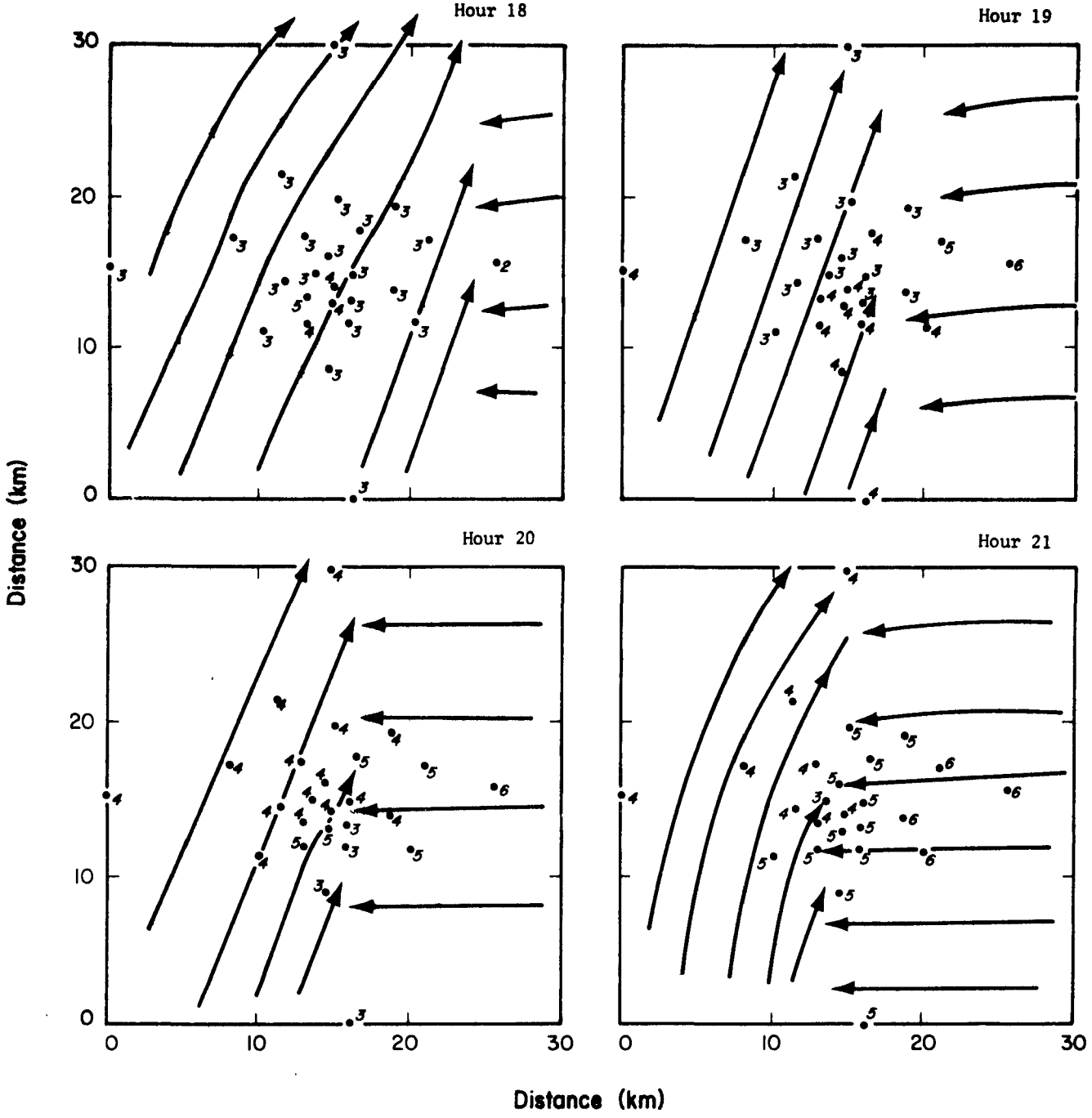

Figure 2-8 Wind Fields Used in RAM Case Study - Numbers indicate wind speed (m/s); arrows indicate wind direction at observing stations (•). Configuration of stations simulates RAPS network.

75I3I8

A comparison of multiple- and single-station model runs reveals that the locations of areas of maximum concentration are different. The results of the multi-station cases show that the location of maximum concentration occurs in the vicinity of the sea breeze front, in the area where onshore and offshore flow patterns converge. The movement of the front inland causes the zone of maximum concentration to move roughly in concert with the front because the pollutant material which is emitted completely in the southwest corner of the grid is no longer transported to the northeast unimpeded. Observations during lake breeze cases along Lake Michigan confirm the existence of a concentration maximum at the sea breeze front (Lyons, 1972). It should be noted, however, that this is due to the fumigation of elevated plumes as well as surface confluence in the wind field. In the single station case, the meteorological conditions for the whole region are given by the observations at a single point. This being the case, the pattern of model calculated concentrations undergoes a dramatic change within one hour in response to the 180° shift in wind direction with the passage of the sea breeze at one point. When multiple-station data are included, the shift in pollutant pattern is more smooth and gradual. In the absence of suitable field data, no definitive assessment of the accuracy of these modifications can be made. However, the use of multi-station data produces results which are in reasonable agreement with expected values.

2.2 SCIM

2.2.1 Description of Model

The purpose of SCIM is to provide a method of estimating the air quality characteristics of a particular pollutant over a specified area from randomly sampled hourly concentration values in order to estimate the frequency of short-term concentrations and the mean long-term concentration. Conventional emission inventory data in the form of the Implementation Planning Program (IPP) data and standard weather data in the form of punched cards or magnetic tape from the National Weather Service (NWS) are used as input data. The historical sequence of hourly or 3-hourly surface observations and twice daily upper air meteorologi-

cal data is sampled at pre-specified time intervals to provide the meteorological setting for the conventional Gaussian plume calculations to follow. Concentrations due to point and area source emissions are determined at preselected receptor points. Thus, a sample of hourly concentrations is obtained for the period of meteorological record. Statistical techniques due to Larsen (1972) are implemented to determine the frequency distribution of pollutant concentrations as well as the long-term mean concentration.

Concentrations due to point source emissions, χ_p, are determined from the standard Gaussian plume equation with a chemical decay term:

$$\chi_p = \frac{Q}{2\pi u\, \sigma_y(x)\, \sigma_z(x)} \exp\left\{-\frac{1}{2}\left(\frac{y}{\sigma_y(x)}\right)^2 - \frac{kx}{u}\right\}\left[\exp\left\{-\frac{1}{2}\left(\frac{H-z}{\sigma_z(x)}\right)^2\right\} + \exp\left\{-\frac{1}{2}\left(\frac{H+z}{\sigma_z(x)}\right)^2\right\}\right] \qquad (2\text{-}12)$$

where

χ_p = pollutant concentration due to point source emissions, g m^{-3}

Q = pollutant emission rate at source, g sec^{-1}

u = wind speed, m sec^{-1}

$\sigma_y(x)$ = horizontal diffusion parameter, m

$\sigma_z(x)$ = vertical diffusion parameter, m

H = effective height of the source, m

y = crosswind distance between source and receptor, m

x = downwind distance from source to receptor, m

z = height of receptor above ground or reference level, m

k = chemical decay constant, sec^{-1}

Whereas in RAM the horizontal and vertical standard deviations of the plume σ_y and σ_z are given as functions of travel time, in SCIM these

quantities are specified as the more conventional functions of downwind distance. The relationships used in SCIM are those given by McElroy (1969) for urban areas and those given by Turner (1970) for rural areas.

Calder's (1971) narrow plume hypothesis is invoked for the process of identifying those area sources contributing to pollutant concentrations. The concentration, χ_A, at a single receptor from all area sources is

$$\chi_A = \frac{1}{\sqrt{2\pi}} \int_0^{x_d} \frac{\bar{q}(x)}{u\sigma_z(x)} \exp\left(-\frac{kx}{u}\right) \left[\exp\left\{ -\frac{1}{2}\left[\frac{H-z}{\sigma_z(x)}\right]^2 \right\} + \exp\left\{ -\frac{1}{2}\left[\frac{H+z}{\sigma_z(x)}\right]^2 \right\} \right] dx \qquad (2\text{-}13)$$

where

q = pollutant emission rate from area sources, g m^{-2} sec^{1}

x_d = distance from receptor to upwind edge of the source area, m

Only area sources whose boundaries intersect the upwind azimuth of a receptor are considered.

The Briggs (1969) formulation of plume rise is used to determine effective plume height.

The vertical wind speed variation is given by a power law whose exponent is a function of Turner-Pasquill atmospheric stability class. A unique feature of SCIM is that time varying patterns of emissions are linked to the chronology of weather observations, so that variations in emission rates and in dispersive processes are accounted for. In the emission algorithm, the emission rates are related to ambient air temperature and time of day, a feature which is especially applicable where emissions are related to space-heating requirements.

The need for the incorporation of multi-station data input exists when continuous meteorological observations are available from several sites within the same region.

The modifications to SCIM were developed on the assumption that the complete input requirements of the present single-station version of SCIM are met at one station and that observations only of wind direction and speed exist at the other stations. The specific algorithm modifications consist of changes in the calculation of Briggs' plume rise and point- and area-source pollutant contributions. Since plume growth is a function of downwind distance, many of the modifications are simpler and more straightforward than the parallel changes required for RAM.

2.2.2 Modifications to SCIM

In order to incorporate multi-station data input, changes were made to SCIM in the following model areas:

- Plume Rise
- Ventilation Wind
- Plume Configuration For Point Sources
- Plume Configuration For Area Sources
- Pollutant Decay

2.2.2.1 Plume Rise

As in RAM, the modification to the calculation of plume rise in SCIM is to use the wind speed at the source as determined by one of the techniques discussed in Section 3.

2.2.2.2 Ventilation Wind

Similarly, the wind speed at the source is used for u in the denominator of Equation 2-12. Thus, u can vary from location to location in the multiple station case.

2.2.2.3 Plume Configuration for Point Sources

The plume centerline azimuth is defined as the wind direction calculated at the midpoint of the line joining the source-receptor pair, and thus varies from pair to pair. The calculation proceeds as in the unmodified version with the determination of downwind and crosswind distance.

2.2.2.4 Plume Configuration for Area Sources

Equation 2-13, which expresses pollutant concentrations due to area source emissions, is an integral of the product of two exponentials and a factor that is inversely related to wind speed along a prescribed path. Also, the integration includes the effect of the vertical dispersion parameter, σ_z, which is a function of downwind distance and stability.

The integration is accomplished in piecewise fashion; the integral is evaluated numerically by the trapezoidal rule on-line intervals in the upwind direction. The length of each integrating interval increases with increasing distance from the receptor in a manner determined internally.

The modifications to SCIM were made in the evaluation of the integral in Equation 2-13: first, the upwind direction is taken to be the average wind direction over the plume path interval, and second, the wind speed u is taken to be the average wind speed over that path. Since wind direction and speed may vary over the path of the plume in the multi-station case, the integration is accomplished on a series of connected line segments that approximates a curved path. The value of wind speed used varies from interval to interval in response to changing wind conditions.

This modification to SCIM is shown schematically in Figure 2-9. The integration begins at the receptor location R. The location B upwind of R is determined by using the wind direction at R as the azimuth and the internally prescribed integration interval for distance. A new location B' is then determined by using the wind direction at A, the midpoint of the segment RB, as the azimuth for the upwind direction. The selection of wind conditions at A as the average wind conditions affecting plume travel in the first upwind interval yields a reasonable first-order approximation to the actual plume conditions. The wind speed at A is used for u in the denominator of the integrand in Equation 2-13. In the next upwind integration interval, points C and C', corresponding to the first and second guesses of upwind direction, are virtually coincident because the wind field varies little over that

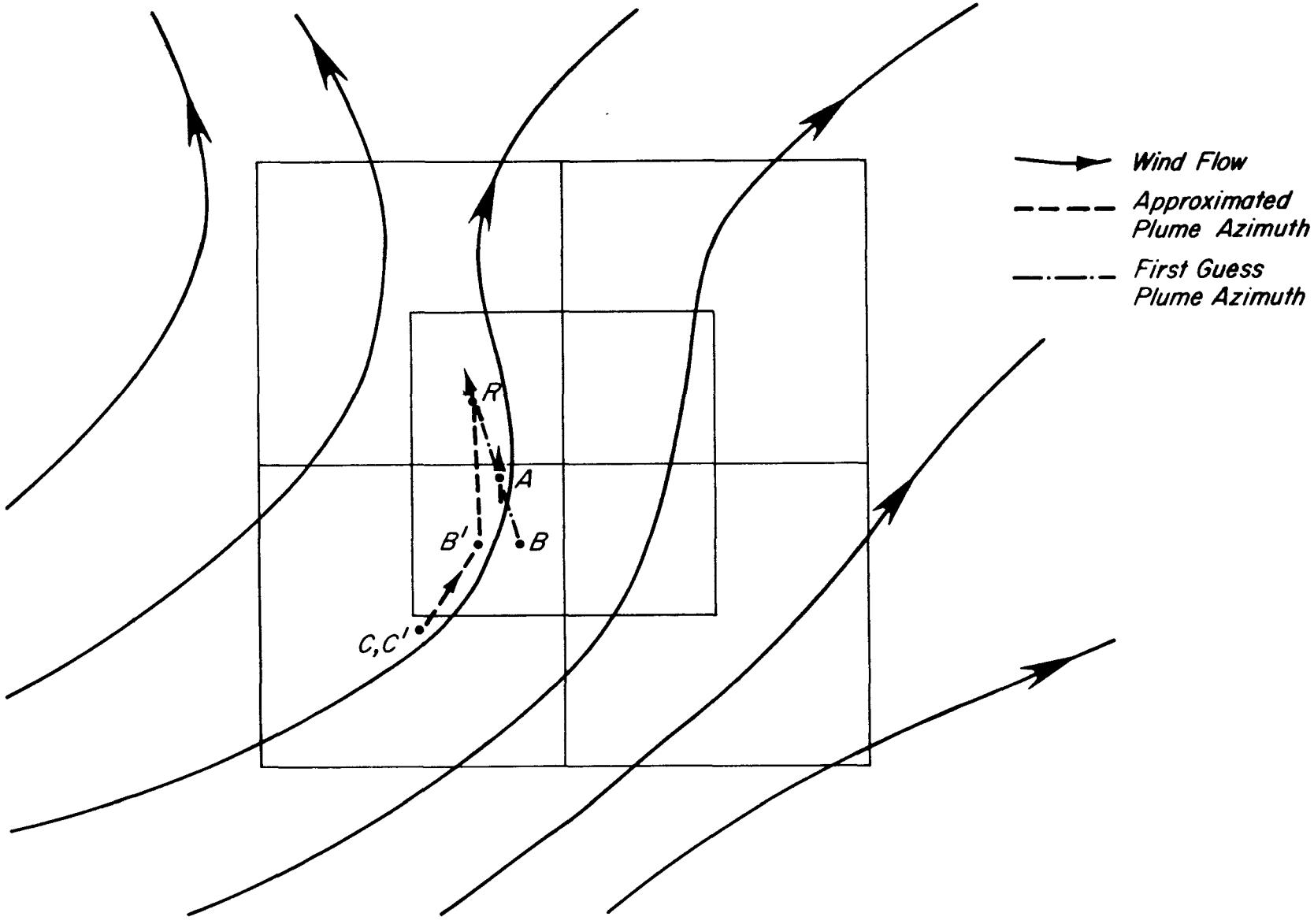

Figure 2-9 Plume Path for Area Source in SCIM - R is receptor; final plume path is line RB'C'. A is mid-point of first guess plume path RB.

interval. It may be expected in the general case that the wind field will vary little over some integration intervals. The process is repeated until the desired upwind integration distance has been achieved.

2.2.2.5 Pollutant Decay

SCIM incorporates the effect of chemical decay of the pollutant and physical transformation from one species to another. The half-life of pollutant decay rate, k (Equation 2-13), is input externally, and the amount of chemical decay is determined by the travel time experienced by the plume. Since travel time t is given by the ratio of downwind distance to wind speed,

$$t = \frac{x}{u} \qquad (2\text{-}14)$$

it is necessary to determine the appropriate wind speed in the multiple station case.

For point sources, the term x in Equation 2-14 in the multi-station version is the downwind distance determined for the particular source-receptor pair by the method described in Section 2.2.2.3. The wind speed at the mid-point of the line segment joining the source-receptor pair is used for u.

2.2.3 Model Case Study

Three runs were made with SCIM for the purpose of illustrating the changes. The emissions inventory and the locations of receptors and observation stations that were used for all of these runs are shown in Figure 2-10. The emissions inventory was designed so that the model results could be readily interpreted. Four area sources of varying strengths are located symmetrically on the grid. In addition there are five point sources, one of which is located at the center of the modeled area. The point sources were assumed to have low stacks so that non-zero pollutant concentrations could be assured at the four receptor locations, each at the center of an area source. The dimensions of the square grid were set at 10 km on a side.

For the single station SCIM calculations, a series of 3-hourly surface National Weather Service observations from El Paso, Texas for

Point Sources

	Ht. (m)	Emission Rate (grams sec^{-1})
P1	20	5000
P2	15	2500
P3	15	1000
P4	15	800
P5	10	200

Area Sources

	Ht. (m)	Emission Rate ($\mu g\ m^{-2}\ sec^{-1}$)
A1	10	1
A2	20	8
A3	20	2
A4	10	4

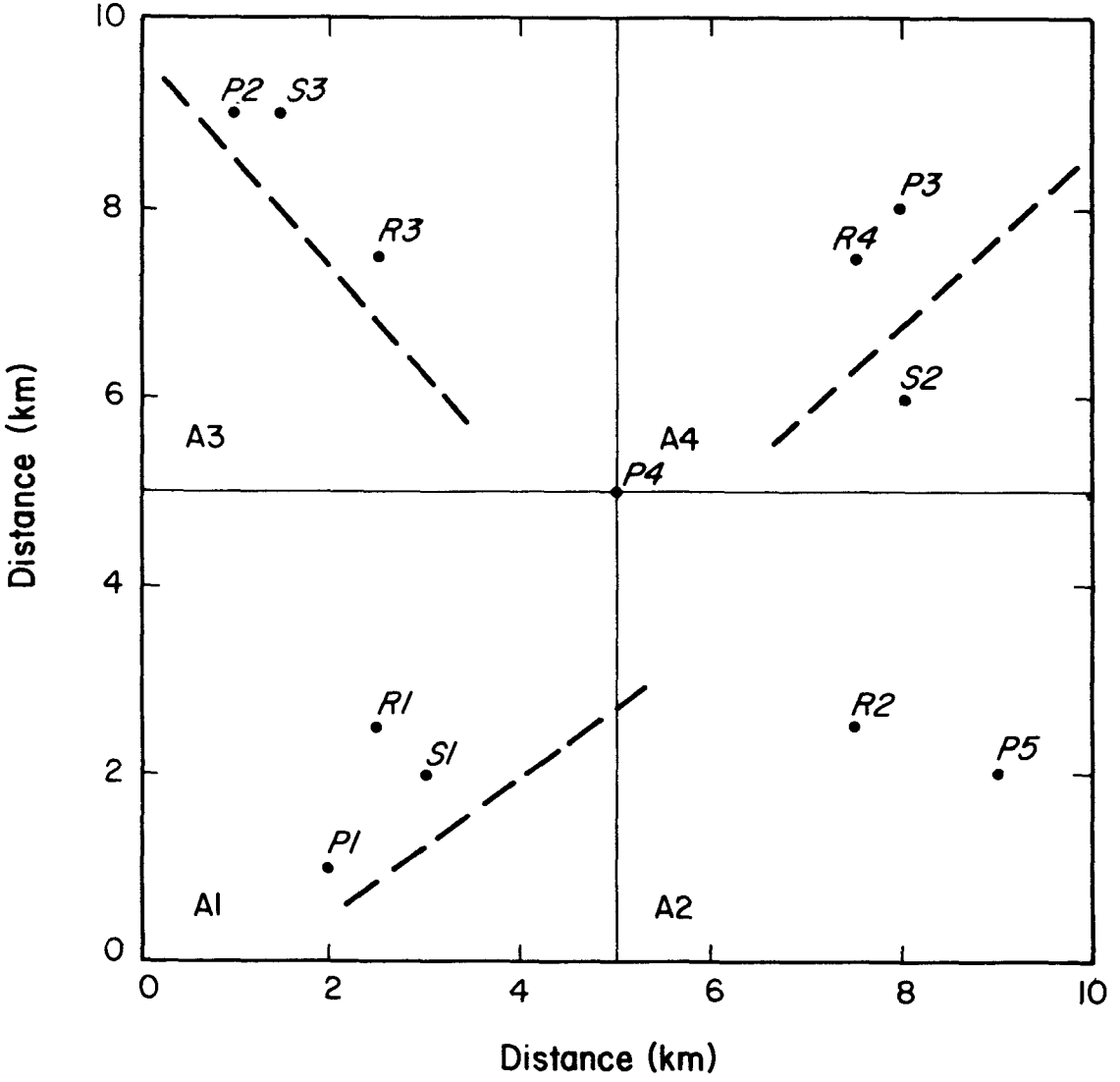

Figure 2-10 Emissions Inventory Used in SCIM Case Study - R1, R2, R3 and R4 are receptor locations; S1; S2 and S3 are meteorological station locations; ____ ____ ____ indicates axis of topographic barrier.

the period 0200 on 1 March through 1100 on 4 March 1971 were used. Since suitable upper air data were not available in time for this calculation, it was assumed that the morning mixing depth was 500 m and the afternoon depth 1500 m on all days. The wind observations at El Paso for the period are shown as Station #1 in Table 2-2 and at location S1 in Figure 2-10.

The hypothetical wind data for the multi-station case was developed for Stations S2 and S3 in Figure 2-10 for the hours modeled. It was assumed that wind conditions at S2 and S3 were similar to those observed at S1 except that topographical barriers, indicated by dashed lines in Figure 2-10, caused channeling and/or blockage of the wind, depending on the orientation of the S1 wind with respect to the barriers. This would result in an increase or decrease in the wind speed depending on the wind direction and orientation of nearby barriers. An appropriate change in wind direction was also made based on the same considerations. The results of this are shown in Table 2-2.

A test of programming accuracy was performed on a multiple station case by assigning Station 1 data to all three stations. This run duplicated the results of the single-station case.

A comparison of the multiple station case with all 3 stations used for meteorological input and a single station case with only Station 1 is made in Table 2-3. The multi-station case was run using a selective angle of 45° (see Section 3.1.2). The results at receptor 1 are very similar for both cases due to the close proximity of this receptor to Station 1. The effect of the multiple-station data can be seen most readily at the other three receptors. For instance, during the hour ending at 1700 on 1 March, the wind speed and direction at Station 3 are markedly different than the wind conditions at Station 1 because of the topographic barrier just to the west of the station, which blocks the wind from that direction. As a result, the wind speed at sources P4 and P2 are lower in the multi-station case and yields higher pollutant concentration at receptors R2 and R4 than in the single-station case. Receptor 3 shows increased impact from source P2 because of wind shifts to the northwest and a decrease in wind speed at Station 3. During hour 0500 on 3 March, however, the concentrations are decreased at all receptors in the multi-station case because of increased wind speed away from

TABLE 2-2

MULTIPLE STATION WIND INPUT FOR SCIM

WD = Wind Direction, Tens of Degrees

WS = Wind Speed, Knots

Month, Day, Hour	Station 1 (El Paso Data)		Station 2		Station 3	
	WD	WS	WD	WS	WD	WS
30102	35	05	33	04	35	07
30105	15	06	15	07	14	07
30108	36	05	02	04	36	06
30111	16	10	16	12	15	10
30114	24	15	24	17	30	05
30117	27	28	26	23	31	06
30120	33	13	31	08	33	14
30123	31	14	30	07	31	13
30202	30	22	29	16	31	15
30205	30	15	29	10	31	10
30208	29	17	28	14	30	10
30211	34	10	01	05	34	10
30214	03	11	03	10	03	12
30217	02	09	02	08	02	10
30220	02	06	02	07	02	08
30223	12	07	12	09	12	10
30302	12	03	12	05	12	08
30305	12	03	12	05	12	08
30308	00	00	18	01	00	00
30311	18	03	18	05	18	03
30314	00	00	18	02	18	03
30317	24	08	24	10	20	04
30320	24	06	24	08	20	03
30323	04	04	04	04	04	05
30403	00	00	08	02	07	05
30405	08	03	08	06	08	06
30408	01	03	03	03	02	06
30411	17	03	18	06	17	08

TABLE 2-3

MULTIPLE AND SINGLE STATION SCIM CONCENTRATIONS, $\mu g\ m^{-3}$

Month,Day,Hour	Single Station Run Receptor				Multiple Station Run Receptor			
	R1	R2	R3	R4	R1	R2	R3	R4
30102	54.0	42.9	170.1	111.1	45.8	31.3	180.7	113.6
30105	78.3	206.1	250.6	259.3	78.0	202.7	228.1	224.1
30108	56.6	59.0	210.8	157.2	55.1	50.4	262.1	182.8
30111	16.5	25.2	63.6	60.5	16.4	26.1	58.2	51.6
30114	7.8	10.8	33.2	26.3	8.2	31.4	33.7	28.4
30117	4.7	6.8	17.4	15.2	5.1	27.0	19.6	33.7
30120	22.8	23.5	78.3	56.3	23.1	22.0	90.8	73.7
30123	13.9	18.1	49.3	39.1	14.7	19.5	63.5	58.4
30202	7.1	9.5	26.2	21.7	7.5	14.5	31.1	29.3
30205	16.0	21.8	61.1	50.5	17.1	34.3	75.1	72.4
30208	21.0	29.4	80.9	69.1	22.3	48.4	91.3	93.8
30211	19.0	19.9	64.4	50.1	19.7	20.2	118.4	87.4
30214	23.3	19.2	56.9	42.5	23.5	18.0	61.0	45.3
30217	61.4	39.2	135.2	89.1	60.6	36.0	148.4	95.8
30220	160.7	87.0	323.4	198.2	137.3	66.9	279.0	168.4
30223	117.1	167.7	169.8	125.0	110.0	132.0	140.6	97.2
30302	226.8	325.2	329.2	242.3	192.1	189.1	211.9	143.6
30305	400.5	574.3	581.3	427.8	339.1	333.9	374.1	253.4
30308 Calm*								
30311	26.7	36.0	160.2	137.0	26.4	33.5	123.6	88.0
30314 Calm*								
30317	20.0	27.9	87.6	69.2	20.7	41.2	86.2	64.7
30320	38.4	53.2	171.2	138.8	39.7	79.5	165.6	126.9
30323	196.6	111.7	276.3	209.5	190.9	94.2	273.9	202.2
30402 Calm*								
30405	494.7	371.8	533.2	367.8	330.6	196.0	301.3	185.6
30408	109.3	108.3	364.5	271.2	100.8	61.5	347.8	243.4
30411	24.7	31.8	121.2	103.4	24.0	18.4	75.1	54.3

* Cases of calm winds are not considered by SCIM and are deleted from the sample.

Station 1. This kind of analytic reasoning can be extended for every hour of the modeling period to account for differences between single-station and multi-station calculations.

For typical applications of SCIM it would be desirable to select a sampling interval not divisible into 24 rather than the three-hour interval chosen here so that all hours of the day would be sampled. However, in order to obtain a sample large enough to allow the application of Larsen's statistical techniques from a limited historical record, a short sampling interval was used. The results of the statistical techniques in the form of frequency distributions are shown in Tables 2-4 and 2-5. Comparable geometric means of pollutant concentration are obtained for both cases with significantly higher arithmetic means and standard deviations for the single-station case. This indicates a wider range of concentrations in the single-station case with a few hours of much higher and lower values. An inspection of the results in Table 2-3 bears this out. These results are purely a function of the specific inputs provided and are not expected to be generally true.

TABLE 2-4

SCIM OUTPUT FOR SINGLE STATION CASE

CUMULATIVE FREQUENCY DISTRIBUTION OF CALCULATED SO2 CONCENTRATIONS (UG/CU.M)

PERCENTILE	RECEPTOR 1	2	3	4	5
HIGH	494.7	574.3	581.3	427.8	581.3
99.5	482.9	549.0	575.3	420.3	577.8
99.0	471.1	523.7	569.3	412.8	574.3
95.0	357.1	360.2	491.0	343.7	400.5
90.0	211.7	265.6	346.8	265.2	325.2
80.0	117.1	111.7	276.3	209.5	206.1
70.0	69.8	73.0	191.0	148.0	138.8
60.0	54.0	42.9	169.8	125.0	103.4
50.0	25.7	33.9	128.2	96.3	63.6
40.0	22.8	27.9	80.9	69.1	50.5
30.0	19.5	22.6	64.0	53.4	31.8
20.0	16.0	19.2	56.9	42.5	22.8
10.0	7.5	10.2	29.7	24.0	16.5
5.0	5.3	7.5	19.6	16.9	9.5
1.0	4.7	6.8	17.4	15.2	4.7
0.5	4.7	6.8	17.4	15.2	4.7
LOW	4.7	6.8	17.4	15.2	4.7

LAST RECEPTOR SHOWS DISTRIBUTION FOR ALL RECEPTORS COMBINED

REGION 1 STATISTICAL SUMMARY FOR SO2

RECEPTOR	X	Y	CASES	MEAN	STANDARD DEV.	MOMENTS 2ND	3RD	4TH	GEOMETRIC MEAN	S.DEV.
1	2.5	2.5	25	88.7	124.5	0.227E 05	0.851E 07	0.363E 10	41.4	3.493
2	2.5	7.5	25	97.1	138.0	0.277E 05	0.117E 08	0.568E 10	47.4	3.236
3	7.5	2.5	25	176.6	152.4	0.535E 05	0.215E 08	0.100E 11	121.6	2.531
4	7.5	7.5	25	133.5	110.1	0.295E 05	0.850E 07	0.283E 10	94.7	2.434
ALL			100	124.0	134.8	0.334E 05	0.126E 08	0.555E 10	69.0	3.158

TABLE 2-5

SCIM OUTPUT FOR MULTIPLE STATION CASE

CUMULATIVE FREQUENCY DISTRIBUTION OF CALCULATED SO2 CONCENTRATIONS (UG/CU.M)

PERCENTILE	RECEPTOR 1	2	3	4	5
HIGH	339.1	333.9	374.1	253.4	374.1
99.5	338.0	317.5	370.8	252.1	361.0
99.0	337.0	301.1	367.5	250.9	347.8
95.0	296.0	201.0	336.2	238.6	301.3
90.0	191.5	192.6	290.2	213.1	243.4
80.0	110.0	94.2	262.1	182.8	185.6
70.0	69.3	64.2	196.3	135.2	126.9
60.0	45.8	48.4	148.4	97.2	91.3
50.0	25.2	35.2	121.0	90.9	72.4
40.0	23.1	31.4	90.8	73.7	54.3
30.0	20.2	26.5	75.1	61.5	33.7
20.0	16.4	20.2	61.0	51.6	26.1
10.0	7.8	18.2	32.4	31.5	19.5
5.0	5.7	15.4	22.5	28.7	14.7
1.0	5.1	14.5	19.6	28.4	5.1
0.5	5.1	14.5	19.6	28.4	5.1
LOW	5.1	14.5	19.6	28.4	5.1

LAST RECEPTOR SHOWS DISTRIBUTION FOR ALL RECEPTORS COMBINED

REGION 1 STATISTICAL SUMMARY FOR SO2

RECEPTOR	X	Y	CASES	MEAN	STANDARD DEV.	MOMENTS 2ND	3RD	4TH	GEOMETRIC MEAN	S.DEV.
1	2.5	2.5	25	76.3	94.4	0.144E 05	0.381E 07	0.114E 10	40.1	3.199
2	2.5	7.5	25	73.1	79.0	0.113E 05	0.258E 07	0.694E 09	48.3	2.406
3	7.5	2.5	25	153.6	104.1	0.340E 05	0.909E 07	0.268E 10	118.2	2.214
4	7.5	7.5	25	112.7	69.0	0.173E 05	0.319E 07	0.650E 09	92.9	1.926
ALL			100	104.0	92.4	0.193E 05	0.467E 07	0.129E 10	67.9	2.683

2.3 CDM

2.3.1 Brief Description

The purpose of CDM is to calculate long-term pollutant concentrations for time periods of several months and longer from emissions inventory data and the joint frequency distribution of observed wind direction, wind speed and atmospheric stability classes. The usual application is in urban areas for non-reactive pollutants.

For point sources, the average concentration, χ_p and χ_A, due to point sources and area sources respectively, is

$$\chi_p = \frac{16}{2\pi} \sum_{n=1}^{N} \sum_{\ell=1}^{6} \sum_{m=1}^{6} \frac{\phi(k_n, \ell, m)\, Q_n\, S(\rho_n, z; U_\ell, P_m)}{\rho_n} \qquad (2\text{-}15)$$

$$\chi_A = \frac{16}{2\pi} \int_0^\infty \sum_{k=1}^{16} q_k(\rho) \sum_{\ell=1}^{6} \sum_{m=1}^{6} \phi(k,\ell,m)\, S(\rho, z; U_\ell, P_m)\, d\rho \qquad (2\text{-}16)$$

where

N = number of point sources

k_n = wind sector appropriate to the nth point source

k = index identifying wind direction sector

Q_n = emission rate of the nth point source

ρ = distance from the receptor to an infinitesimal area source

$q_k(\rho)$ = $Q_A(\rho, \theta)\, d\theta$ for the k^{th} sector where $Q_A(\rho, \theta)$ is emission rate of the area source at distance ρ per unit area and unit time

ρ_n = distance from the receptor to the nth point source

ϕ = joint frequency function

m = index identifying the Pasquill stability class

ℓ = index specifying wind speed

$S(\rho,z; U_\ell, P_m)$ = dispersion function defined below

z = height of receptor above ground level

U_ℓ = representative wind speed

P_m = Pasquill stability category

If the receptor is presumed to be at ground level (z=0), the functional form of $S(\rho_n, 0; U_\ell, P_m)$ is

$$S(\rho, 0; U_\ell, P_m) = \frac{2}{\sqrt{2\pi}\, U_\ell \sigma_z(\rho)} \exp\left[-\frac{1}{2}\left(\frac{H}{\sigma_z(\rho)}\right)^2\right] \exp\left[\frac{-0.692\ \rho}{U_\ell\ T_{1/2}}\right] \quad (2\text{-}17)$$

if $\sigma_z(\rho) \leq 0.8L$; or

$$S(\rho, 0; U_\ell, P_m) = \frac{1}{U_\ell L} \exp\left[\frac{-0.692\ X}{U_\ell\ T_{1/2}}\right] \quad (2\text{-}18)$$

if $\sigma_z(\rho) > 0.8L$

with

$\sigma_z(\rho)$ = vertical dispersion function

H = effective stack height of source distribution

L = afternoon mixing height

$T_{1/2}$ = assumed half-life of pollutant, hours

Removal by physical and chemical processes is incorporated by the expression $\exp\left[\frac{-0.692\ \rho}{U_\ell\ T_{1/2}}\right]$. The total concentration for the averaging period is the sum of concentrations due to the point and area source emissions for the period.

The vertical dispersion parameter, $\sigma_z(x)$, is given by a power-law expression ax^b+c, where a, b and c are empirical constants that are functions of stability and downwind distance. The use of Pasquill-Turner stability classes has been modified to account for urban heat island effects, which are particularly important during the nighttime hours. Plume rise is given by Briggs (1971). The calculation of area-source contributions is made by selecting only those sources lying directly upwind of a given receptor.

The modifications implemented in the CDM to incorporate multiple-station data input were addressed to situations in which joint frequency distributions of wind direction, wind speed, and atmospheric stability class (wind roses) are available at several locations within a region. This often occurs in metropolitan areas serviced by several airports at which NWS meteorological stations exist, such as New York City or Chicago. The same situation also exists at the site of comprehensive urban field experiments such as the St. Louis RAPS, where instrumented towers are continuously recording meteorological variables. The description of the modifications to CDM to accept this type of data input follows.

2.3.2 Modifications to CDM

The modification to CDM involved the derivation of a new joint frequency distribution of weather classes on the basis of inverse distance power law weighting of the individual weather class frequencies from the wind roses included. Thus, the frequency of occurrence of a given weather class f_i is

$$f_i = \frac{\sum_{j=1}^{N} A_j g_{ij}}{\sum_{j=1}^{N} A_j} \qquad (2\text{-}19)$$

where

N = the number of stations for which wind roses are included

A_j = weighting factor

g_{ij} = frequency of occurrence of weather class i at station j

The same options are available in this method as exist for RAM and SCIM in the selection of weighting factors, A_j, in the wind field generator technique. In addition, the exponent of the power law desired in the inverse distance weighting can be varied as described in Section 3.

The calculation of long-term pollutant concentration is unaffected; the Gaussian-plume calculation proceeds with the same parameters for each weather class considered as in the unaltered model. The modification occurs when the frequency of occurrence of the class is used to

weight the calculated pollutant concentration in order to obtain the long-term means. The frequency of occurrence of an individual class will vary from place to place in response to the proximity to observation locations.

2.3.3 Example of CDM Run Utilizing Model Modifications

Several test runs were made using the modified version for CDM. The unmodified model was run with the input shown in Appendix C for 3 simulated day-night STAR wind roses for Newark, New Jersey (EWR), John F. Kennedy (JFK) and LaGuardia Airports (LGA) in New York City. This case was chosen as representative of the type for which the CDM modifications would be most applicable, e.g., an urban area in which climatological wind roses are available at several locations.

A comparison was made using model runs of each wind rose separately as a single-station case and together as a multiple-station case. The selective angle method with θ equal to 45 degrees was used. The relative position of the airports was estimated and superimposed on a 900 square kilometer grid (Figure 2-11). The wind roses are given in Appendix C-3.

The model results are shown in Table 2-6. The mean concentrations at receptors 10, 18 and 7 are the same as the corresponding single-station calculation using the observation point closest to that location, JFK, LGA and EWR respectively. For the remaining sector points, the mean concentrations reflect proximity to each of the three stations. Although the wind roses are similar, differences of more than 25 percent occur between the results of the single-station and multi-station runs.

Area (A) and Point (P) Sources

	Emission Rate (g/m^2/sec for A) (g/sec for P)	Ht. (m)
A1	25.2	10.
A2	25.2	10.
A3	63.0	15.
A4	63.0	15.
A5	159.6	25.
A6	63.0	20.
A7	63.0	20.
P1	4987.5	200.
P2	997.5	100.
P3	997.5	100.
P4	997.5	100.
P5	199.5	50.

Stations

S1	JFK
S2	LaGuardia
S3	Newark

x = Receptor Location

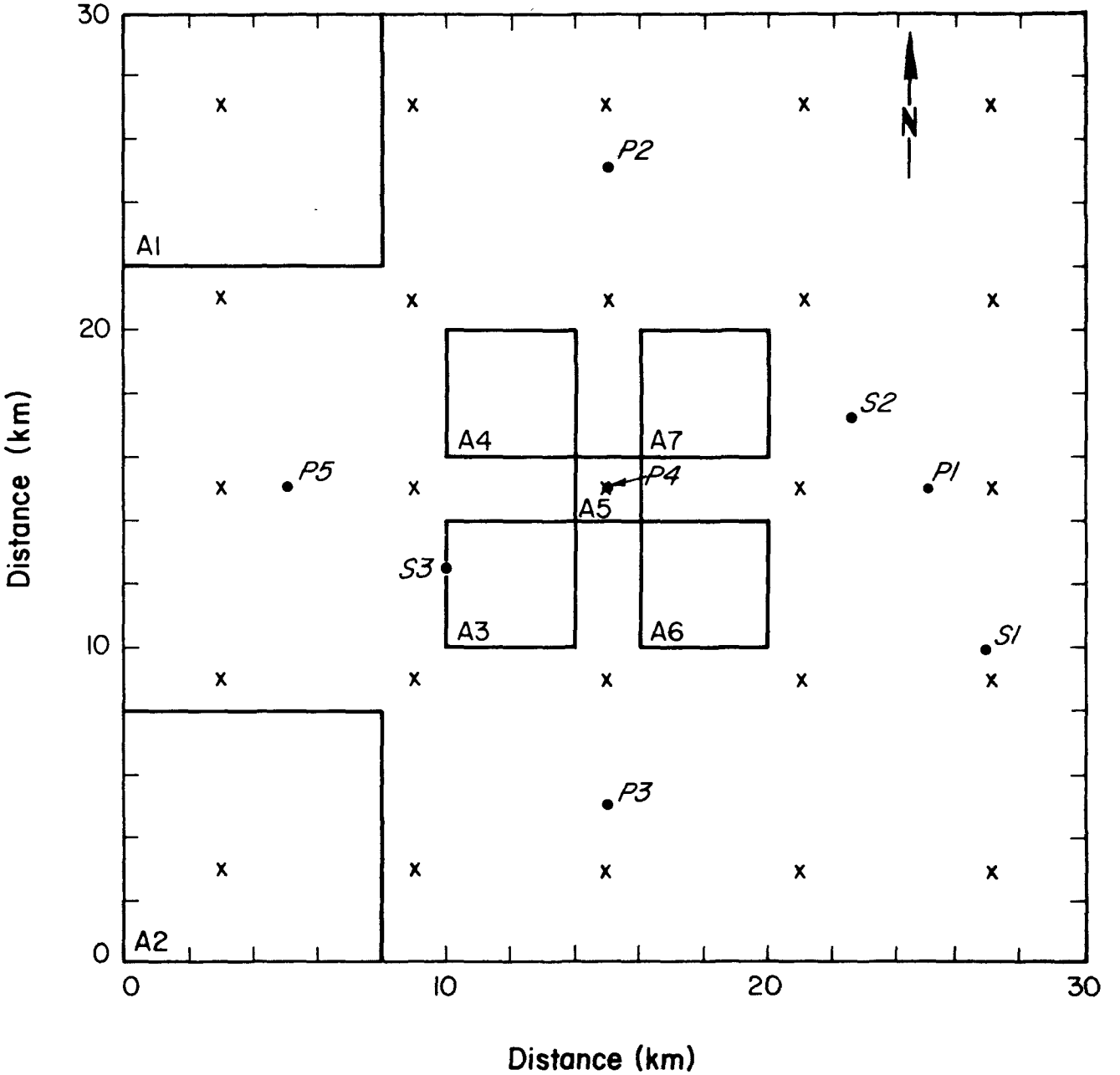

Figure 2-11 Emissions Inventory, Meteorological Station and Receptor Locations Used in CDM Case Study

TABLE 2-6

COMPARISON OF CDM RESULTS

Receptor #	Receptor Coordinates, Km		Receptor Cencentrations, $\mu g\ m^{-3}$ Wind Rose Used			
	x	y	JFK	LGA	EWR	Multi-station Case
1	3	3	13	15	14	14
2	9	3	9	12	11	11
3	15	3	8	9	7	8
4	21	3	8	9	9	8
5	27	3	9	9	7	9
6	3	9	8	10	8	8
7	9	9	12	15	15	15
8	15	9	19	19	15	16
9	21	9	14	15	15	14
10	27	9	8	11	9	8
11	3	15	7	7	5	5
12	9	15	14	14	14	14
13	15	15	136	136	157	149
14	21	15	18	18	21	18
15	27	15	9	9	9	9
16	3	21	6	7	7	7
17	9	21	8	8	9	8
18	15	21	21	16	16	16
19	21	21	14	13	22	13
20	27	21	9	8	10	8
21	3	27	12	11	11	11
22	9	27	7	6	8	7
23	15	27	12	7	4	7
24	21	27	8	6	7	7
25	27	27	12	8	7	9

Station:	Locations:	x	y
JFK		26.75	10.00
LGA		22.50	17.25
EWR		10.00	12.75

3. TECHNIQUES FOR GENERATING WIND FIELDS

The preceding chapter describes the steps in the diffusion calculations at which changes were made in order to accommodate multiple station wind data input. Implicit in the discussion of these changes is the ability to generate the required wind information from the available meteorological observations. The means by which this information is approximated has a critically important effect on the model results. For instance, if the wind conditions at the closest observation point are selected as representative of conditions at a given location, serious errors and discontinuities may develop in the model output if the nearest station is not as representative of the conditions as, for example, a weighted average of several closest stations and that the estimates differ greatly. The meteorological analyst would know how to "draw the contours" in this situation on the basis of his experience with the observed data. In data-sparse areas for example, the analyst will space the isopleths based on his experience and intuition of actual conditions. Any method which is developed to simulate the analyst's product must have the flexibility and capability of accepting new information and experience as it is gained in order to produce a more accurate result.

Several techniques are described for estimating wind speed and direction at any point in a region in which arbitrarily spaced wind observations exist. These methods determine wind direction and speed by interpolating the horizontal orthogonal (u, v) wind components from available data on the basis of inverse-distance power-law weighting. More sophisticated analysis methods that develop analytic expressions for the wind field by minimizing the error in estimating the field while satisfying dynamic relationships between meteorological variables such as wind, temperature, pressure and humidity (e.g. Panofsky, 1949) were considered impractical for the purpose of this study. The primary objection to their use is that they would require generally unfeasible costs for site studies and computer time in order to simulate the complex variations of surface roughness and thermal characteristics, and their effects on the wind flow. This degree of complexity is beyond the scope of EPA's stated goal of "relatively straight-forward modifications" in the basic multiple-source Gaussian plume algorithms.

Four different schemes were developed: the basic inverse distance power-law weighting (IDPL), selective angle (SA), selective radius (SR) and weighting factor matrix (WFM) approach. All are described by the following equation:

$$U_p = \frac{\sum_i U_i F_{ip} / r_{ip}^n}{\sum_i F_{ip} / r_{ip}^n} \qquad (3\text{-}1)$$

where

U_p = parameter value at point p

U_i = parameter value at observation point i

F_{ip} = weighting factor

r_{ip} = distance between p and i

n = exponent of inverse distance power law (n = 1,2,3....)

The difference in methods arises from the specification of i's, the observation points considered in the summation of Equation 3-1, and the values of F_{ip} used.

Since no real data of the type suitable for verification was available, several sets of hypothetical observations were generated for this purpose. Analytically determined scalar fields were superimposed on a grid in which a randomly spaced array of observation points were situated. The field was then sampled throughout the grid utilizing the techniques for generating wind fields. A comparison was made between the estimated values and those calculated from the analytic flow. Two different kinds of analytical fields were used: a constant-gradient, linearly varying field and a physical analogue, potential field of flow around an obstacle.

The results were evaluated on the basis of accuracy, computational efficiency and ease of use. A sensitivity analysis was performed to determine the response to the variation of critical parameters. In the potential flow case the effect of observational error is also investigated. Guidelines for the proper usage of each of the methods are included at the conclusion of this section.

3.1 Description of Methods

3.1.1 IDPL: Inverse Distance Power Law

This method is the most basic and straightforward of the four; all observation points are considered in the summation and $F_{ip} = 1$ for all i and p in Equation 3-1.

3.1.2 SA: The Selective Angle Method

Elimination of redundant or superfluous data is the goal of the selective angle method. The assumption is made that accuracy as well as computation time can be optimized for certain situations by eliminating data determined to contribute little useful information to the calculation of wind conditions at the point in question. In this method, observation stations are selected as inputs to a wind field calculation only if they are the closest stations to the receptor within a specified angular sector. This scheme eliminates the distant stations and leaves a ring of close-by stations around the calculation point.

The first step locates the observation point nearest the calculation point. A pre-selected angle θ bisected by the line connecting the observation station and receptor is constructed (as in Figure 3-1). All points in this sector are eliminated from the summation in Equation 3-1. In Figure 3-1, Stations 2, 3, and 4 are eliminated because they are in the angular sector bisected by Station 1. The process is continued with the closest non-rejected station until all possible sectors have been scanned. The ring of remaining stations then provides the values input to Equation 3-1. The choice of θ determines the maximum number of stations to be included. For instance, if $\theta = 45°$, no more than 8 stations will be considered in Equation 3-1; if $\theta = 360°$, only the closest station will be used.

3.1.3 SR: The Selective Radius Method

The selective radius method, like the SA method, assumes an improvement can be made in accuracy and computational efficiency by eliminating redundant stations. The scheme utilizes the inverse-distance power-law

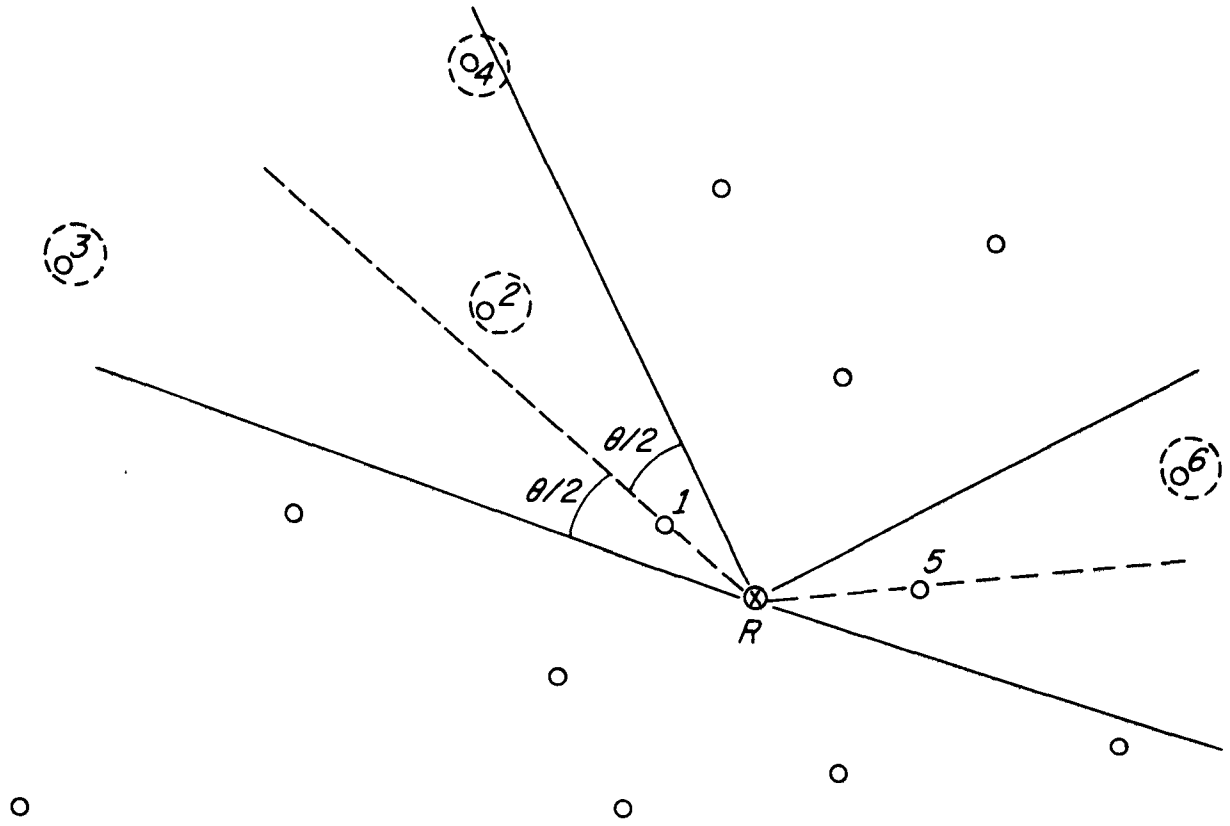

Figure 3-1 Selective Angle Method - R is calculation point; Θ is selective angle. 1 and 5 are included stations; stations surrounded by dashed circles are excluded from calculation. Procedure is repeated for closest station not within angular sectors until all stations have been either included or excluded.

751311

weighting of Equation 3-1. An attempt is made to reduce the degree of redundancy when groups of stations are located close together. These stations may provide a large amount of data while representing only a small portion of the entire wind field. The selective radius method is designed to select one station from each grouping. It also decreases computation time by dealing with a smaller number of stations.

This method is accomplished by first selecting the station closest to the calculation point of interest, location 1 in the example given in Figure 3-2. All stations within a specified radius, r, of that first station (stations 2, 3, 4) are eliminated as inputs. The process is then repeated for the next closest station (station 5, in Figure 3-2) and so on. When all possible eliminations have been made, the remaining stations are included in Equation 3-1 for the calculation of parameter values.

3.1.4 WFM: The Weighting Factor Matrix

This method involves the specification of the array F_{ip} in Equation 3-1. Although the effect of distance is taken into account in the inverse-distance weighting scheme, it may be desirable under certain situations to assign a higher relative weight to one observation point than another, even though both are at comparable distances from the calculation point. This would be the case when a greater amount of confidence is expressed in the quality of a particular set of observations relative to others in the same region. Also, this would occur when topographic or man-made barriers exist within a region, effectively blocking the exchange of air between two adjacent areas and decoupling the atmospheric flow at one location from the other. Even though two locations may be close in terms of separation on a horizontal plane, the wind flow at one place may bear no resemblance to that occurring at the other. In the interpolation scheme, it is necessary to account for this effect when calculating wind conditions in either of these two areas.

The method is implemented by directly inputing the matrix F_{ip}. The p index is given by a grid which divides the modeled region into a maximum of 100 (10 x 10) squares. Thus, in the calculation at the point in grid square p, the weighting associated with observation point i is

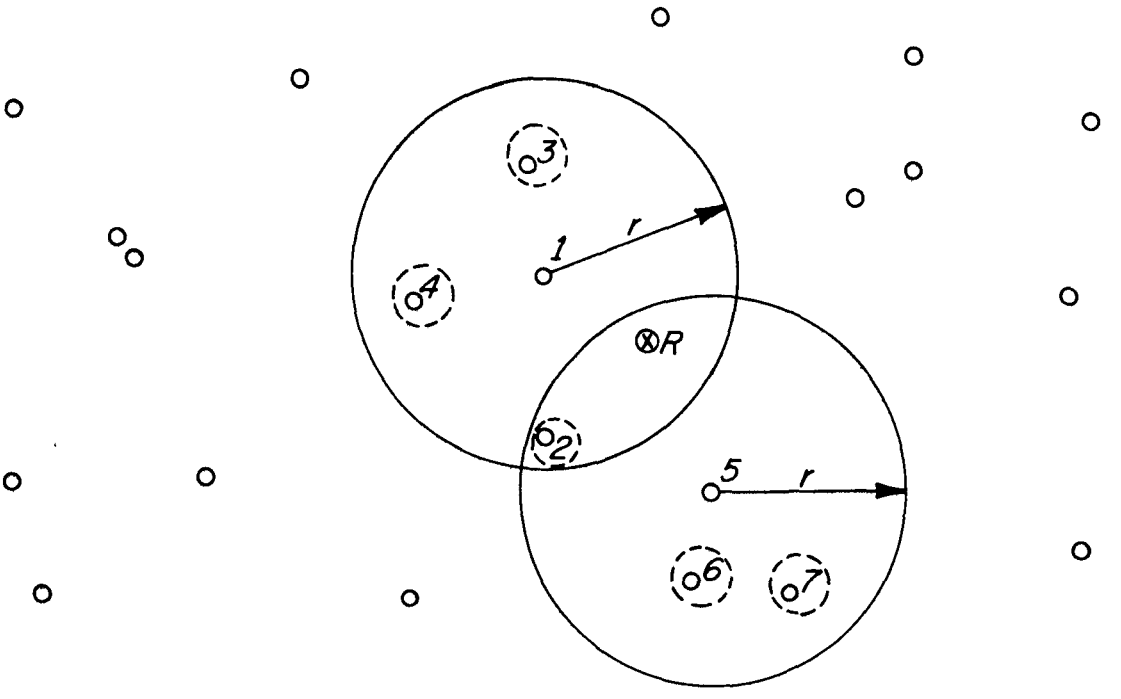

Figure 3-2 Selective Radius Method - R is calculation point; r is selective radius. 1 and 5 are included station points; stations surrounded by dashed circles are excluded from calculation. Procedure is repeated for next closest station not within radii until all stations have been either included or excluded.

751310

F_{ip}. If a weighting factor F_{ip} is set to zero for a particular station-grid square pair, the data from station i is completely eliminated for all calculation points in the p^{th} grid square.

The weighting factor method is the most general of all four methods because it incorporates the largest amount of flexibility. The user can tailor the matrix for the specific case and has a great deal of freedom in doing so. In addition, the weighting factor method can be used in conjunction with any of the other methods. The principal drawback of this method is that the user must be careful in his selection of matrix values and perform a fair amount of preliminary work before implementing this method successfully.

3.2 Analysis of Methods

3.2.1 Methodology

Analytical wind fields were selected so that each of the techniques for generating wind-fields could be evaluated and compared. It is sufficient for this purpose to consider only scalar fields because the wind field vector may be resolved into components that are scalars.

First, a network of observing stations was randomly located on the field. The field was then uniformly sampled at 25 locations, designated as calculation locations, by means of each of the wind-field generator techniques. The weighting factor matrix method was not used because it was assumed that all of the observations were equally representative, i.e., $F_{ip} = 1$ in Equation 3-1 for all i and p. Five, 10 and 20 station networks were used, shown in Figure 3-3 with the calculation locations. Five sets of analytical wind fields were used. Figure 3-4 shows the fields characterized by uniform gradients of parameter values. They are the east-west (EW), north-south (NS), diagonal (D) and circular (C) gradient fields. These patterns were chosen in order that the results of the analysis reflect properties of the schemes themselves and not peculiarities of the wind fields. The linear variations test both orthogonal and transverse directional gradients so that the variation in accuracy of the different methods to gradients in all directions can be determined. The circular case was chosen in order to evaluate the properties of each method in a case where the wind field gradient undergoes a sign reversal.

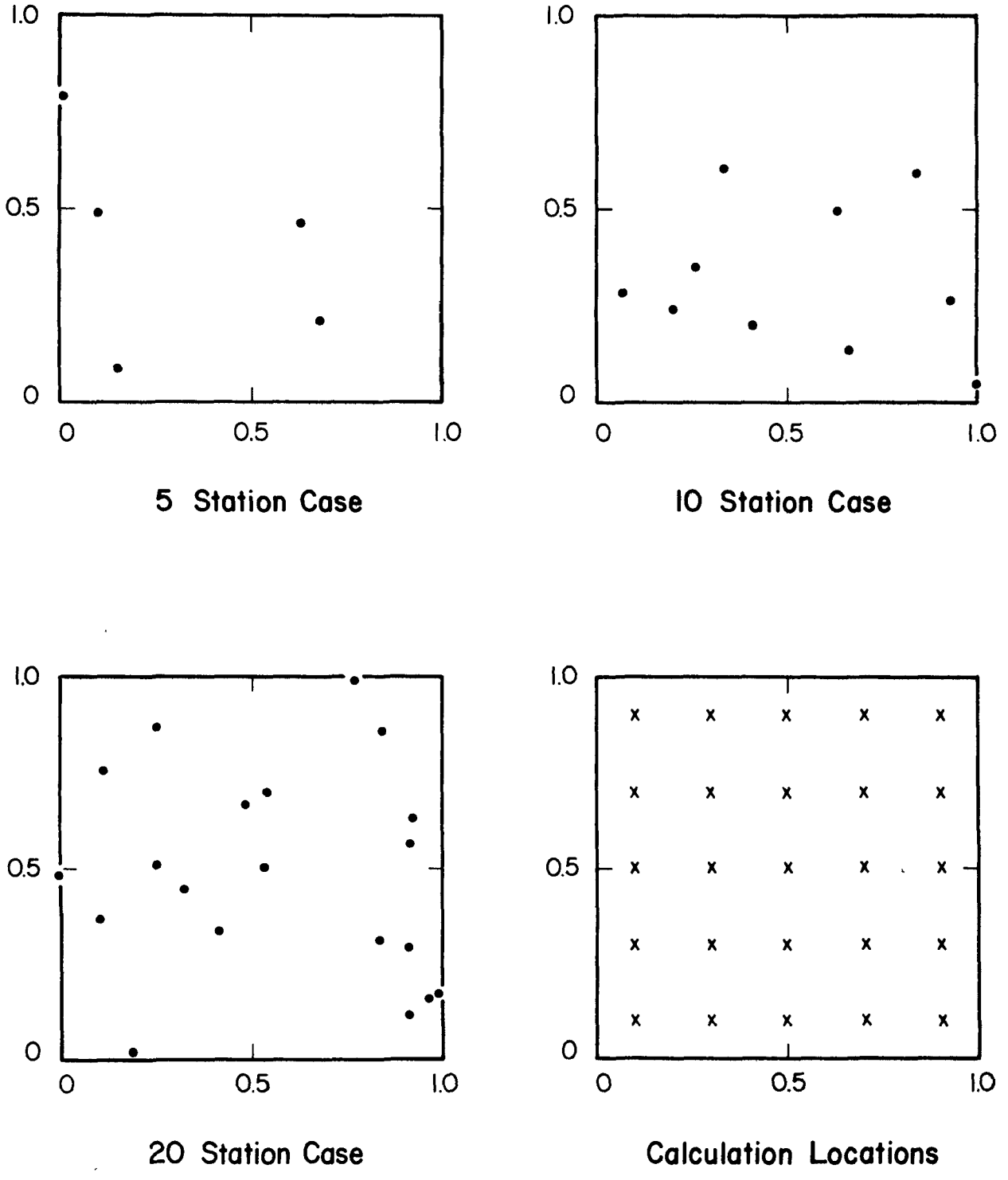

Figure 3-3 Observation Point (•) and Calculation Point (x) Configurations used in comparison of Techniques for Generating Wind Fields

751312

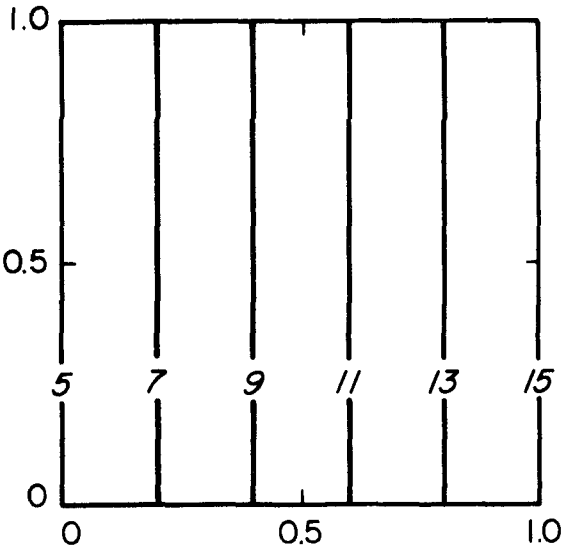

Linear East - West Variation (E-W)

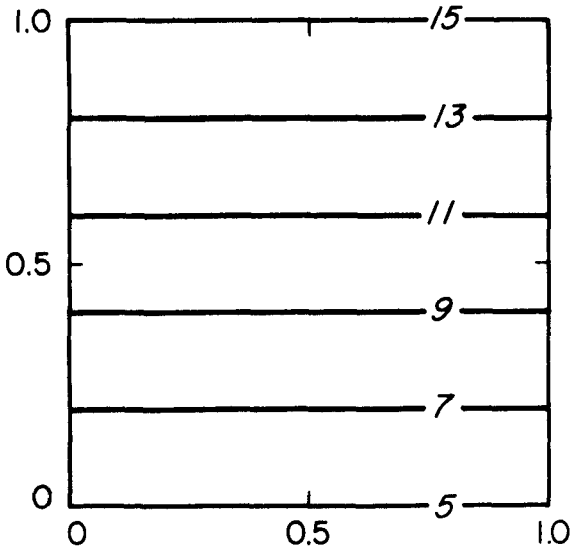

Linear North-South Variation (N-S)

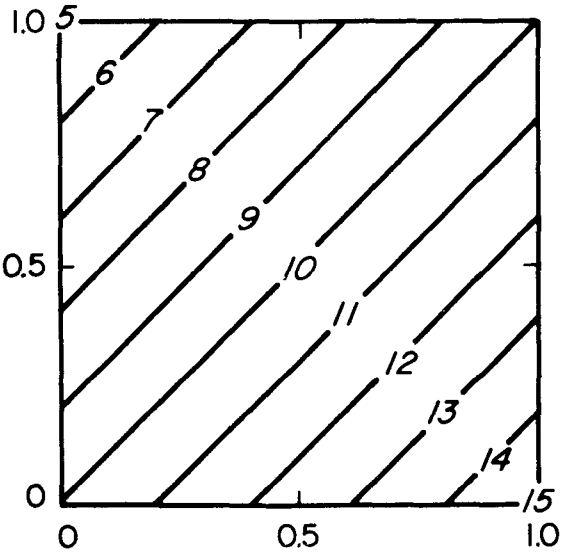

Linear Diagonal Variation (D)

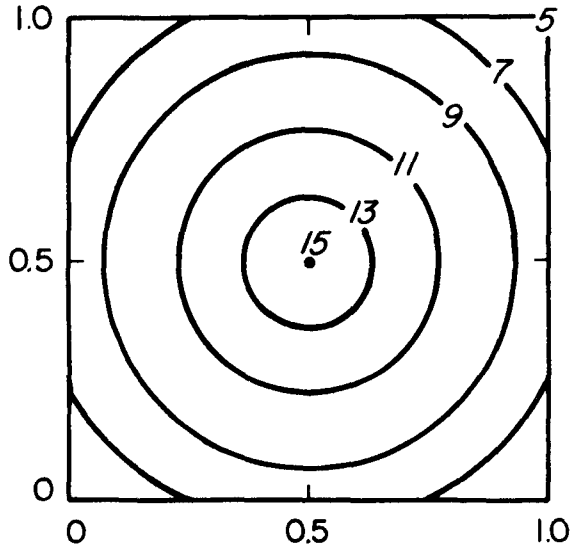

Linear Circular Variation (C)

Figure 3-4 Uniform Gradient, Analytical Wind Fields used in Comparison of Techniques for Generating Wind Fields

751313

The calculated values obtained using the techniques for generating wind fields were compared with the values derived from the analytical expressions describing the wind fields. The root-mean square (RMS) error for all stations was then calculated from:

$$RMS = \sqrt{\sum_i \frac{(A_i - C_i)^2}{N}} \qquad (3\text{-}2)$$

where

A_i = analytically determined value at calculation location i

C_i = calculated parameter value at i

N = 25, the number of calculation points.

An RMS value of zero would indicate perfect replication of the wind field at all points.

3.2.2 Results

A summary of the results of the RMS error analysis is given in Tables 3-1 and 3-2.

Overall, the selective angle method produced the lowest RMS values in both uniform gradient and potential flow cases. In most of the cases this method was successful in minimizing the error regardless of the density of the observation network by eliminating from the calculations the stations which would contribute unnecessary additional information. A ring of stations more or less uniformly distributed about the calculation point remained after the elimination. Generally, the larger the number of observation points, the more complete the areal coverage which should produce more accurate results. This effect, however, was not uniform for all cases studied. In fact, due to the uneven north-south distribution of observation points in the 10 station case, all of the methods exhibited a decrease in accuracy (an increase in the RMS error) in the north-south and diagonal fields in going from 5 to 10 stations. This effect is minimized in the selective angle method. The east-west field shows increases in accuracy with increasing station numbers in all cases. In the 20 station case a further gain in accuracy is achieved by the selective angle technique relative to the other methods.

TABLE 3-1

RESULTS OF R.M.S. ERROR ANALYSIS OF WIND FIELD GENERATOR TECHNIQUES, UNIFORM GRADIENT FIELDS

N is power law exponent,
Selective Angle is 45°,
Selective radius is 1/10 of the grid length

Wind Field	Method	No. of Observation Points		
		5	10	20
East-West	Selective Angle, N=2	1.879	0.948	0.448
	Selective Radius, N=2	1.966	1.364	0.906
	Inverse Distance, N=2	1.966	1.334	0.979
	Inverse Distance, N=1	2.445	1.880	1.712
	Inverse Distance, N=3	1.742	1.137	0.795
North-South	Selective Angle, N=2	1.719	1.799	0.775
	Selective Radius, N=2	2.167	2.354	1.383
	Inverse Distance, N=2	2.168	2.484	1.450
	Inverse Distance, N=1	2.450	2.864	1.931
	Inverse Distance, N=3	2.062	2.291	1.294
Diagonal	Selective Angle, N=2	0.689	1.107	0.730
	Selective Radius, N=2	0.953	1.372	0.863
	Inverse Distance, N=2	0.953	1.476	1.016
	Inverse Distance, N=1	1.330	1.779	1.401
	Inverse Distance, N=3	0.823	1.347	0.924
Circular	Selective Angle, N=2	1.858	1.844	0.921
	Selective Radius, N=2	1.740	1.756	1.323
	Inverse Distance, N=2	1.740	1.735	1.295
	Inverse Distance, N=1	1.735	1.775	1.591
	Inverse Distance, N=3	1.861	1.830	1.285

TABLE 3-2

R.M.S. ERROR ANALYSIS, POTENTIAL FLOW CASE

N is inverse-distance power law exponent,
25 Calculation Points

		Method:	Inverse Distance N = 2			Selective Angle N = 2	
Case	Component:	u	v	$r = \lvert u^2 + v^2 \rvert^{1/2}$	u	v	$r = \lvert u^2 + v^2 \rvert^{1/2}$
No Error		.345	.556	.447	.172	.353	.259
20% Error		.423	.597	.561	.269	.417	.393

The selective radius method performed with approximately the same accuracy as the non-selective IDPL. Apparently, this method achieved small gains in eliminating from consideration observation points which are very close together. With uneven groupings, the radius length would be suitable for some regions of the study area while being inadequate in others. Stations at relatively large distances would be included while the ring of stations nearest the calculation location would be eliminated. No radius tested produced results as accurate as those produced by the search angle method with a 45° search angle.

In the uniform gradient cases, the effect of varying the power law in the inverse distance weighting was investigated. For the fields used, values of N = 2 and N = 3 produced the best results, with N = 3 holding a slight edge. This can be attributed to the ability of each method to assign a small weight to distant observation points. A $1/r^3$ weighting is more effective in doing this than the $1/r^2$, which in turn is more effective than $1/r$. In the circular case, however, where a reversal in field gradients tends to minimize the penalty in weighting far-away and unnecessary information, the differences in accuracy are smaller.

A second flow field was used to compare the wind field techniques in order to provide an analogue to physically realistic flow situations. Surface flow fields can be very complex, however, they can be approximated to first-order by a non-divergent, irrotational flow which is determined by boundary conditions. A simple case is found in Figure 3-5 where a uniform flow field of 10 m sec^{-1} is perturbed by an obstacle indicated by the stippled area. The striped section of the flow field was chosen as the field for the techniques comparison because the flow varied significantly from one side of the square to the other and would provide for useful, non-trivial results.

The flow field is given by

$$U(x,y) = U + \frac{Mx}{(x-x)_o^2 + (y-y_o)^2} \qquad (3\text{-}3)$$

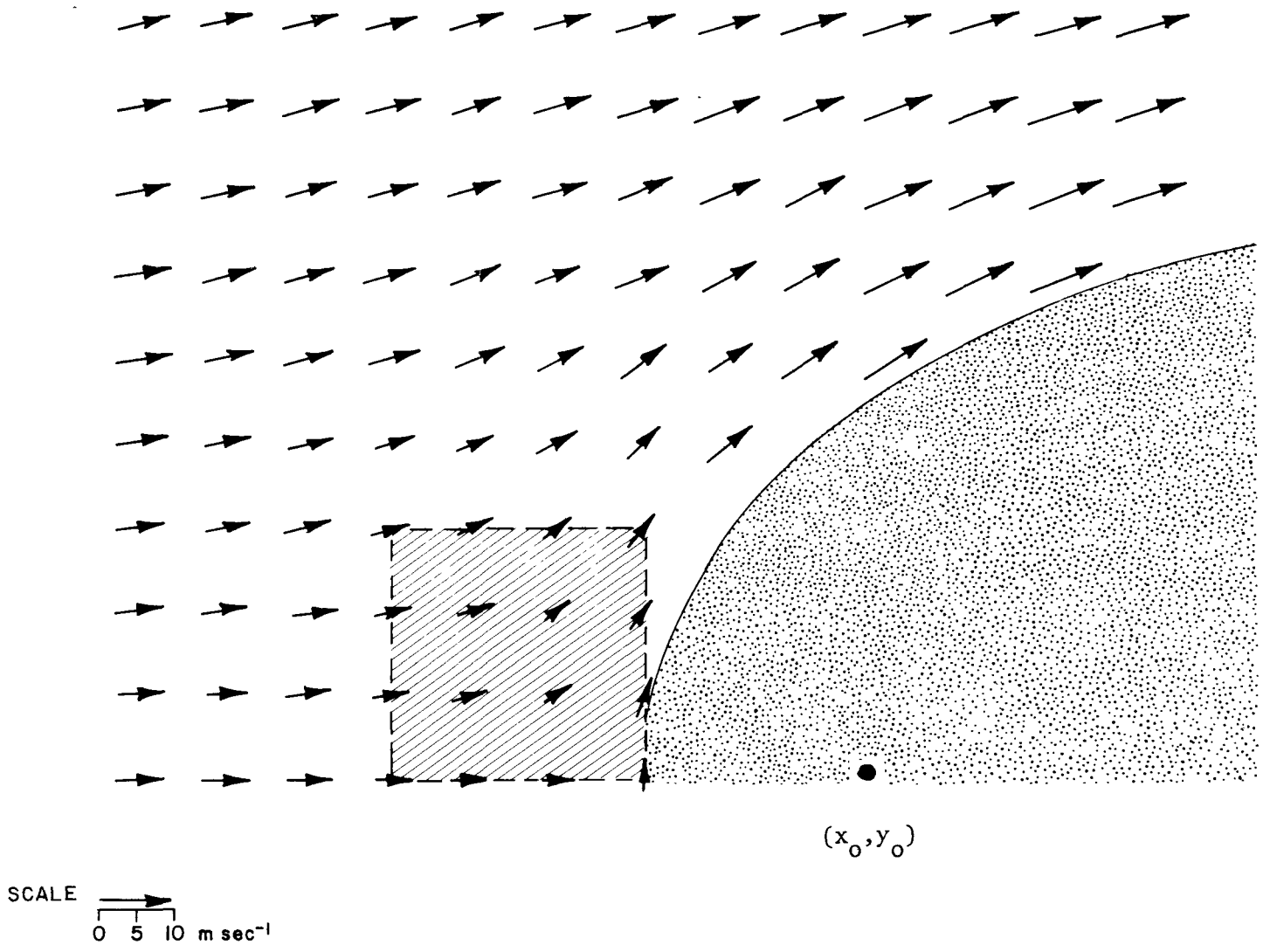

Figure 3-5 Potential Flow Field Used for Comparison of Techniques for Generating Wind Fields - Section used in comparison is striped; obstacle is stippled. Arrows indicate direction of flow; length of arrow is proportional to flow speed. Point (x_o, y_o) is origin of obstacle.

$$v(x,y) = \frac{My}{(x-x_o)^2 + (y-y_o)^2} \qquad (3\text{-}4)$$

where

M = obstacle parameter which determines the shape and size of the obstacle = 3×10^4 m^2 sec^{-1} in this case

x,y = cartesian space coordinates

x_o, y_o = coordinates of "origin" of obstacle, shown in Figure 3-5 for this case

U = velocity of unperturbed flow = 10 m sec^{-1} in this case.

In the potential flow field case the selective angle method generates the most accurate values (Table 3-2). A second potential flow case was studied in order to determine the effect of error in observations on the accuracy of the wind field generating methods. At each of the observation points the true wind condition is known from the analytic expression which describes the field Equations 3-3 and 3-4. A random error is introduced to the true wind condition varying to a maximum of 20% of the actual value. This new value is then used for the station observation.

The effect of this error on the performance of the wind generator schemes is not immediately evident from the results in Table 3-2. One would expect that the non-selective IDPL weighting would gain in accuracy relative to the selective angle because the effect of large error at any one location is minimized by including all stations. It is possible for the selective angle method to lose in accuracy by providing values which are biased by the error at any one of the included stations. The gain in accuracy by the non-selective scheme is shown to a small degree in Table 3-2, in which the selective angle method is shown to have a 73% advantage in RMS error in predicting the flow speed r in the no-error case but only a 43% advantage in the 20% error case.

3.3 Other Considerations and Guidelines for Use

Several different methods have been presented, and it is important that the user select the one that is most suitable for his particular

case. Each method is used in conjunction with the model modifications described in Section 2 involving the diffusion calculations. The main considerations are accuracy, computational efficiency and ease of use.

The results of the analytical wind fields analysis indicate that the search angle technique is the most accurate given a relatively dense network of observation stations and reasonably accurate observations. An inverse-square distance power-law which is the most frequently used for applications of this sort should be adequate for most purposes but it may be desirable to use a higher power law where gradients are large. If accuracy of the observations is low and the density of stations is moderate, it may be preferable to use a non-selective power law weighting utilizing an N = 3 power law in order to average the error effect and still assign small weights to far away stations. The selective radius technique is most accurate in cases where a cluster of stations surrounds a calculation point and only the parameter value at the closest station is desired to represent conditions at the calculation point. Thus, situations where the density of monitoring stations is uneven would be candidates for the use of this method.

All of the above considerations can be accounted for in the weighting factor matrix (WFM) method. Variability in the reliability and accuracy of the observation field can be included in the assignment of relative matrix weights. All stations are first considered as if they were at comparable distances. Then each would be compared on the basis of its areal representativeness and observational reliability. Finally, the weights are assigned on the basis of the user's judgment of the relative weight of these factors. It may be useful to establish a matrix and then inspect the model results obtained to see if changes could be made to increase the accuracy of the method. One way to establish the matrix values is to establish regression relationships between observations at a point and the network of stations surrounding that point. A large amount of historical data and a relatively large network would be required. The explained variance at a location due to each of the other stations could then be used as a guide in assigning weights to the stations.

The WFM method has the capability for incorporating the effect of natural and/or man-made obstructions to airflow. For example, a zero weight would be assigned to an observation station if a location on the

opposite side of a topographic barrier were being considered. The effect of tall buildings and urban heat island could likewise be included.

The WFM method is the most difficult to use because of the large amount of preparatory work required. A poorly selected matrix would be reflected in the model results. On the other hand, non-selective methods that do not discriminate between possible included stations are easily implemented and can be used in a straightforward manner. After some consideration of the nature of the available data network, it should be possible to obtain more accurate results from either of the two selective schemes.

The use of any of these methods carries with it a penalty in computer time. At any point in the program at which data from the interpolation schemes is required, a subroutine is called to produce the desired value. In the non-selective IDPL method all stations are included in the calculation. A reduction in calculation time is achieved by selecting a smaller number of stations, but a compensating effect results from the logic used to achieve the elimination. The amount of computer time required for a particular run will thus depend on the number of stations input, because of the number of calculations and eliminations to be achieved, and on the size of the emissions inventory, because that determines the number of times wind generator schemes are used.

The actual amount of computer time varies with the system efficiency. However, an example of the amount of computer time used in a RAM application on an IBM 360/75 system is illustrative. When the model was run for a small emissions inventory (Figure 2-4b) for the single station cases, 2 minutes of execution time was required to run for 24 hours, or 5 seconds per hour. Using the search angle method in a multi-station case with 25 stations and θ equal to 45° required 30 seconds of time for an hour; with θ = 360° (selecting only the closest station), 20 seconds was used. This time was increased dramatically to 120 seconds for one hour's calculation using the non-selective IDPL weighting.

4. CONCLUSIONS AND RECOMMENDATIONS FOR FUTURE WORK

Modifications that allow the utilization of multiple-station wind data input were implemented in three standard Gaussian-plume models. The short-term models, RAM and SCIM, were modified so that a series of concurrent wind observations at several locations can be input. The model results in the multi-station cases show the effect of horizontal variability in the wind fields. Modifications of the long-term model, CDM, involved the use of joint frequency distributions of weather classes, or wind roses obtained at several locations to determine an interpolated wind rose for the desired location intermediate or adjacent to the observation points. The modifications involved essentially two parts of the programs; the determination of the proper parametric value from discrete observation points using a wind field generator and the alteration of dispersion calculations (only in SCIM and RAM) to incorporate the effects of a varying wind field. In cases where a continuous wind field is available from an external source, such as a numerical flow model, the results can be used directly in the dispersion models.

Since all of the modifications are relatively straightforward, the simplifications limit their application to situations where the variations in the wind field are approximately of the same horizontal length as the average source-receptor distance. Where the source-receptor separation is large, this may not be valid. However, in these cases pollutant concentrations will often be low because of large distance separation. More sophisticated mathematical treatments not practical in the present study would be required to handle highly perturbed fields accurately.

The results of case studies utilizing generated model input indicate that the model predictions in the multiple-station case were more reasonable than those obtained using the unmodified single-station version. In RAM, the series of hourly concentration values showed a uniform transition from one pattern to another as a sea breeze front moved across the region. The corresponding single-station calculation showed an abrupt change in concentration patterns with the passage of the front. It was clear that in this case a single wind vector was a poor representation of the total flow field. The SCIM case study described a situation where consistent deviations in wind conditions due to

topographic effects resulted in changes of model estimates of frequency distributions of pollutant concentration in the direction that would be expected. Wind roses compiled from wind observations at locations within the same region were used to illustrate the changes implemented in CDM. Model predictions in the multi-station case differed somewhat from the single-station cases, in which each of the three wind roses was used separately. Since the wind roses were fairly similar these differences were not large; however, they showed the advantage of using multi-station wind rose input over the selection of a single wind rose to represent conditions over a whole region.

No verification was done during this program because suitable input data was not available. It is anticipated that with the establishment of the St. Louis RAPS a large amount of multi-station wind data suitable for verification of all the models will become available. It can then be determined which of the implemented changes best describes urban area diffusion and how these changes are to be used on a continuing basis. Also, as experience is gained with the collection and analysis of St. Louis data it should become apparent which of the various parameters, particularly the establishment of the weighting factor matrix, should be selected to yield the most accurate results.

Another item which requires further investigation is the development of plume trajectories in curved wind fields. One approach is to define the wind field explicitly by relatively simple balanced equations. These methods fit analytic expressions, usually in the form of a power series, to observed data so that the difference between calculated and observed values is minimized. It should be possible to develop simple mathematical treatments which are sufficiently accurate for the flows encountered in the St. Louis RAPS once enough data has been collected. More exact plume trajectories could then be constructed than are presently practical by means of interpolation techniques.

5. REFERENCES

Briggs, G. A., 1969: Plume Rise, U.S. Atomic Energy Comm., Div. of Tech. Info., NTIS Pub. No. TID-25075.

_____, 1971: Some Recent Analyses of Plume Rise Observation, pp. 1029-1032, in Proc. Sec. Intl. Clean Air Congress, ed. H.M. Englund and W.T. Berry, Academic Press, New York.

Calder, R. L., 1971: A Climatological Model for Multiple Source Urban Air Pollution, 33 pp. in Proc. 2nd Meeting of the Expert Panel on Air Pollution Modeling, NATO Committee on the Challenges of Modern Society, Paris, France, July 1971.

Larsen, R. I., 1971: A Mathematical Model for Relating Air Quality Measurements to Air Quality Standards, Environmental Protection Agency, Office of Air Programs, Research Triangle Park, N.C. 1971.

McElroy, J. L., 1969: A Comparative Study of Urban and Rural Dispersion, J. App. Meteorology, 8, 19-31.

Panofsky, H., 1949: Objective Weather Map Analysis, J. Meteorology, 6, 386-392.

Turner, D. B., 1970: Workbook of Atmospheric Dispersion Estimates, U.S. Dept. of Health, Education, and Welfare, National Air Pollution Control Administration, Cincinnati, Ohio.

Turner, D. B. and J. Hrenko, 1974: RAM: Real-Time Air-Quality-Simulation Model, U.S. Environmental Protection Agency, Research Triangle Park, N.C., 170 pp. (unpublished).

TECHNICAL REPORT DATA

(Please read Instructions on the reverse before completing)

1 REPORT NO.	2.	3. RECIPIENT'S ACCESSION NO.
21AD0-36		

4. TITLE AND SUBTITLE	5. REPORT DATE
Adaptation of Gaussian Plume Model to Incorporate Multiple Station Data Input, Volume 1	June 1975
	6. PERFORMING ORGANIZATION CODE

7 AUTHOR(S)	8. PERFORMING ORGANIZATION REPORT NO.
Harvey S. Rosenblum, Bruce A. Egan, Michael J. Keefe, Claire S. Ingersoll	ERT P-1121

9. PERFORMING ORGANIZATION NAME AND ADDRESS	10. PROGRAM ELEMENT NO.
Environmental Research & Technology, Inc. 696 Virginia Road Concord, Massachusetts 01742	1AA009
	11. CONTRACT/GRANT NO.
	EPA-68-02-1753

12. SPONSORING AGENCY NAME AND ADDRESS	13. TYPE OF REPORT AND PERIOD COVERED
United States Environmental Protection Agency Office of Research & Development Washington, D. C. 20460	Final Report
	14. SPONSORING AGENCY CODE

15. SUPPLEMENTARY NOTES

16. ABSTRACT

EPA urban dispersion models were modified to consider multiple station information on wind speed and direction. Three models were modified: the Real-Time Air-Quality-Simulation Model (RAM) and the Sampled-Chronological Input Model (SCIM), both short-term averaging models, and the Climatological Dispersion Model (CDM), a long term averaging model. Relatively straight forward modifications, which are useful and practical approximations have been made. The modifications had two basic objectives: the first, to develop techniques for describing wind conditions at any point within a region in which arbitrarily-located observing points exist; and second, to identify critical points in the dispersion algorithms at which the additional multiple-station wind data could be incorporated and to modify these computation routines accordingly. The modifications were compared among themselves on the basis of accuracy, computational efficiency and ease of use. Although no observational data was available to verify the various approaches, the results of applications to hypothetical meteorological situations indicate that more realistic results can be obtained by the incorporation of multiple-station data.

17. KEY WORDS AND DOCUMENT ANALYSIS

a. DESCRIPTORS	b. IDENTIFIERS/OPEN ENDED TERMS	c. COSATI Field/Group

18. DISTRIBUTION STATEMENT	19. SECURITY CLASS *(This Report)*	21. NO. OF PAGES
	20. SECURITY CLASS *(This page)*	22. PRICE

EPA Form 2220-1 (9-73)